TECHNICAL REPORT NO. LWL-CR-04-P-73

AERIAL RECONNAISSANCE BINOCULARS

USALWL TASK 04-P-73

by

R. Lambert
General Electric Co.
Space Sciences Laboratory

June 1974

Final Report

Contract No. DAAD05-74-C-0734

APPROVED FOR PUBLIC RELEASE; DISTRIBUTION UNLIMITED

U.S. ARMY LAND WARFARE LABORATORY

Aberdeen Proving Ground, Maryland 21005

The findings in this report are not to be construed as an official Department of the Army position unless so designated by other authorized documents.

The contents of this report are not to be used for advertising, publication, or promotional purposes. Citation of trade names does not constitute an official endorsement or approval of the use of such commercial products.

REPORT DOCUMENTATION PAGE		READ INSTRUCTIONS BEFORE COMPLETING FORM
1. REPORT NUMBER TECHNICAL REPORT NO. LWL-CR-04P-73	2. GOVT ACCESSION NO.	3. RECIPIENT'S CATALOG NUMBER
4. TITLE (and Subtitle) Aerial Reconnaissance Binoculars		5. TYPE OF REPORT & PERIOD COVERED Final Report
		6. PERFORMING ORG. REPORT NUMBER
7. AUTHOR(s) R. Lambert General Electric Company		8. CONTRACT OR GRANT NUMBER(s) DAAD05-74-C-0734
9. PERFORMING ORGANIZATION NAME AND ADDRESS General Electric Company PO Box 8555 Philadelphia, PA 19101		10. PROGRAM ELEMENT, PROJECT, TASK AREA & WORK UNIT NUMBERS USALWL Task 04-P-73
11. CONTROLLING OFFICE NAME AND ADDRESS US Army Land Warfare Laboratory Aberdeen Proving Ground, MD 21005		12. REPORT DATE June 1974
		13. NUMBER OF PAGES
14. MONITORING AGENCY NAME & ADDRESS(if different from Controlling Office)		15. SECURITY CLASS. (of this report) UNCLASSIFIED
		15a. DECLASSIFICATION/DOWNGRADING SCHEDULE

16. DISTRIBUTION STATEMENT (of this Report)

APPROVED FOR PUBLIC RELEASE; DISTRIBUTION UNLIMITED

17. DISTRIBUTION STATEMENT (of the abstract entered in Block 20, if different from Report)

N/A

18. SUPPLEMENTARY NOTES

None

19. KEY WORDS (Continue on reverse side if necessary and identify by block number)

20. ABSTRACT (Continue on reverse side if necessary and identify by block number)

The standard military 7x50 binocular is of little use in the detection of targets from severely vibrating platforms such as light aircraft and helicopters. Actively stabilized optical systems are usually large and expensive. Studies have shown that a 3x optical aid is nearly as effective in target detection as are 7x50 binoculars. This report describes the design and fabrication of two pair of 3x binoculars. The important features are a wide field-of-view, 18 degrees, and large exit pupils, 10 mm which should aid in
(CONT)

DD FORM 1 JAN 73 1473 EDITION OF 1 NOV 65 IS OBSOLETE

iii

the detection probability of targets and alleviate problems associated with vibration. Field testing of the optical system is being performed at Fort Hood, TX and the results will be reported separately.

FOREWORD

This effort was sponsored by the US Army Land Warfare Laboratory (USALWL), Applied Physics Branch, under the technical supervison of H. Clay McDowell. This project was designated 04-P-73, Aerial Reconnaissance Binoculars.

TABLE OF CONTENTS

LIST OF ILLUSTRATIONS

LIST OF TABLES

INTRODUCTION

For several years the US Army Land Warfare Laboratory (USALWL) has been developing optical aids for use in high vibration environments where standard military binoculars (7 x 50) are only marginally helpful to the naked eye in the detection of targets. Stabilized optical aids have been developed but they are cumbersome, expensive and of marginal optical quality in many cases. Target acquisition studies, in non-vibrating environments, have shown that low power optical aids are almost as effective as the seven power devices. The lower optical power will alleviate the vibration problem and also permit a wider field-of-view.

A design study was performed by the Muffoletto Optical Company, Inc.* to incorporate the above characteristics together with a large exit pupil and good eye relief into a pair of binoculars for airborne use. The design study was further restricted to incorporate off-the-shelf components to the fullest extent possible, consistent with good optical quality, in order to keep costs reasonable.

This report describes the final design, fabrication and testing of two pair of aerial reconnaissance binoculars based substantially on the previous work. Detail changes in the original optical design were undertaken when computer analysis indicated significant improvement in the overall thru-put at large field angles and an increase in the eye relief.

The project was initiated on March 4, 1974 and the binoculars were delivered on May 28 and June 6, 1974. Presently, one set is undergoing field tests at MASSTER, Fort Hood, Texas. Figure 1 is a photograph of the final binocular design.

*See Appendix A. Reports #1 & 2, Muffoletto Optical Company, Inc., July 2 & October 9, 1973.
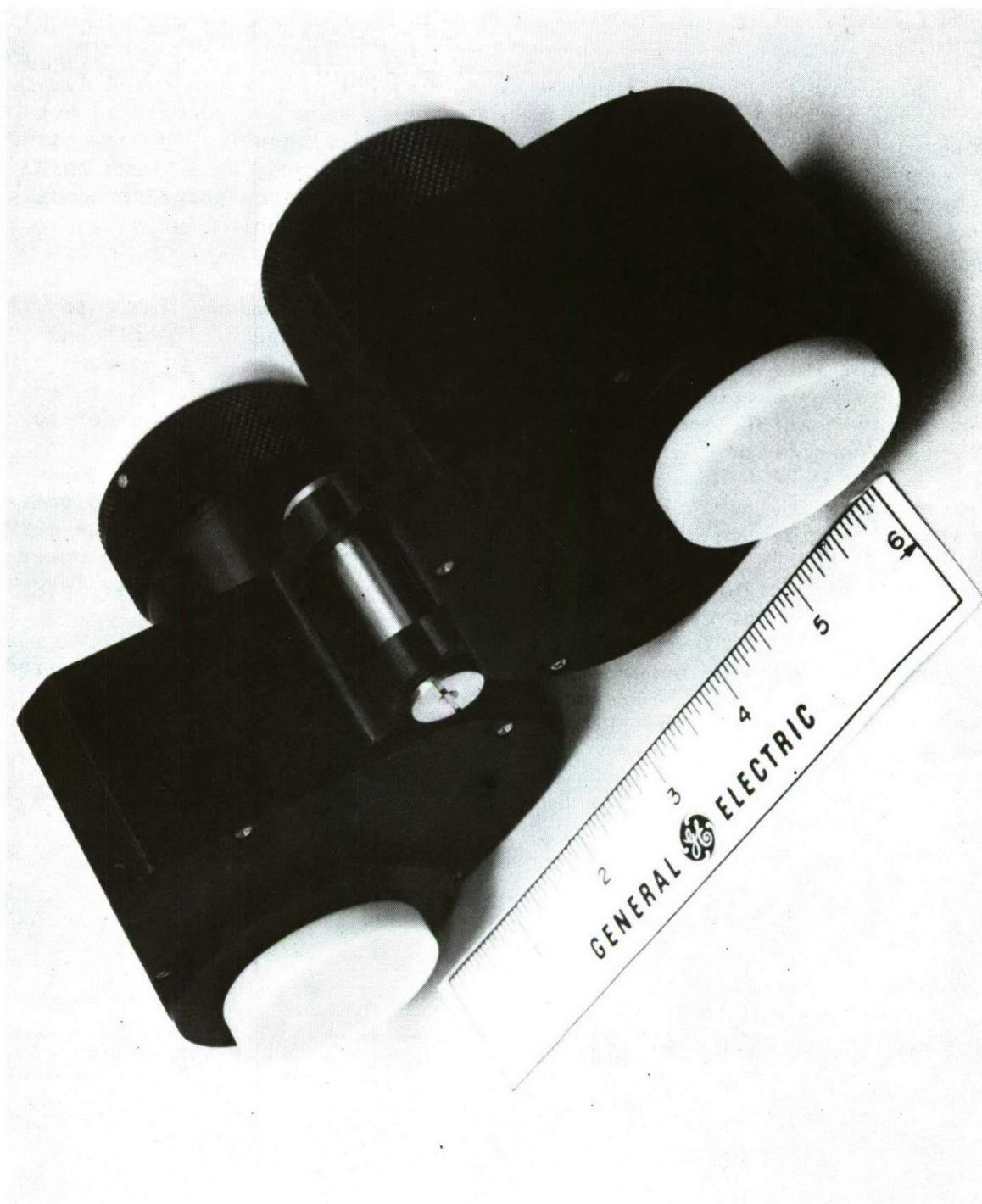
Figure 1. Low Power Binoculars

OPTICAL DESIGN

1. Design Goals

Based on the previous design efforts and the intended system application, the following design goal characteristics for the binoculars were established:

Magnification - 3x

Field-of-view - 20 degrees or greater

Exit pupil - 10 mm

Eye relief - 10-14 mm

Size - as small and as compact as possible

Design & materials - rugged

Components - off-the-shelf, if possible

If all the components were specified and supplied as results of the previous efforts, the only additional design effort required would have been purely mechanical. However, detailed definition of components was not given in the Muffoletto Reports. The reports gave design specifications for the optical components, radii, glass types and component spacings. Implementation of these specifications into hardware resulted in slight variations from the design specifications because of the necessity of placing manufacturing tolerances on all components to be fabricated. The final binocular characteristics were measured and are listed below.

Binocular Characteristics

Magnification	3.1x
Field-of-view	17.8 degrees
Exit Pupil	9.65 mm
Eye Relief	27,4 mm
Size	4.5 x 8.75 x 3.5 inches
Weight	4.3 lbs

3

2. Computer Design - Ray Tracing of Original Design

Initially, it was thought possible to reduce the diameter of the optical elements within the eyepiece in order to reduce their size and weight. The required diameters were not specified. Tables 1.2 and 1.3 of Report #2 show two meridional ray traces through the system but neither represent the extreme ray with respect to the eyepiece. In order to define the required diameter of the eyepiece components, additional ray traces were therefore required.

Initial ray traces on the eyepiece above indicated that the design yielded a nominal 1¼ inch focal length, Erfle design, used in the reversed direction from the originally intended orientation. The eyepieces were available from two vendors, A. Jaegers & Edmund Scientific Co. with identical optical designs but slightly different mechanical designs, the Jaeger model being somewhat larger. The eyepiece contains three cemented doublets. The normal field lens (furthest from the eye) is 0.846 inches (21.48 mm) clear radius, as is the middle element. The normal eye lens (nearest the eye) has a 0.649 inch (16.487 mm) clear radius. Ray traces of the reversed eyepiece design show that for a 30 mm diameter entrance pupil, vignetting will start at a half field angle of 6.3 degrees due to physical blockage at the edge of the first element of the eyepiece. This element also limits the field-of-view to something less than a half angle of 10 degrees regardless of the size of the prisms. This design required a minimum of 33 mm diameter prism assembly in order to prevent vignetting of the 9 degree rays at the edges of the prisms.

Two meridional ray traces are shown in Tables I and II. The nomenclature of each column is as follows:

SURF	An optical surface or plane indexing number
C	The curvature of the plane or 1/radius
T	Linear vertex distance of the next surface
N	Intervening index of refraction
Y	Ray height at SURF
UN	Angle of the ray with the horizontal radians

Surfaces 1 to 6 are the objective lens elements, 7 and 8 the entrance and exit surfaces of the Porro Prism and 9 to 17 the surface of the eyepiece elements. Table I represents a ray starting at the very edge of the objective aperture stop (15 mm) at an angle of - 7.40, which gets vignetted at surface 9, the entrance of the eyepiece since the eyepiece diameter is only 0.649 inches but the ray strikes at - 0.709 inches. Obviously, a ray starting at a steeper negative angle would be vignetted since it would strike surface 9 at a greater radius. Table II shows a ray initiated at - 6.41 degrees which is just barely vignetted at surface 11, the last element of the first cemented doublet. This ray represents the extreme field half angle for which there is no vignetting at the eyepiece. Additional ray

4

TABLE I

Meridional Ray Trace from 15 mm Radius at -7.45 Degrees

SURF	C	T	N	Y	UN
0	0.	0.10000E-03	1.0000	0.59005E+00	-0.13000E+00
1	0.1786	0.20000E+00	1.5167	0.58602E+00	-0.12143E+00
2	-0.2969	0.10000E+00	1.0000	0.57132E+00	-0.28119E+00
3	-0.4454	0.50000E-01	1.6475	0.54795E+00	-0.64086E-01
4	-0.1107	0.10000E+00	1.0000	0.54142E+00	-0.14533E+00
5	0.1852	0.20000E+00	1.5167	0.52873E+00	-0.12872E+00
6	-0.2903	0.10000E+00	1.0000	0.50287E+00	-0.27835E+00
7	0.	0.47500E+01	1.5170	0.46375E+00	-0.16213E+00
8	0.	0.95300E+00	1.0000	-0.41106E+00	-0.27835E+00
9	0.3567	0.87000E-01	1.6490	-0.70948E+00	-0.58041E-01
10	0.8732	0.56500E+00	1.5170	-0.72432E+00	-0.14189E+00
11	-0.5858	0.16000E-01	1.0000	-0.74358E+00	0.25481E-01
12	0.2864	0.10900E+00	1.6490	-0.73604E+00	0.10126E+00
13	0.7032	0.61100E+00	1.5170	-0.71343E+00	0.61591E-01
14	-0.4677	0.20000E-01	1.0000	-0.69474E+00	0.28815E+00
15	0.5587	0.57200E+00	1.5170	-0.62143E+00	0.31081E+00
16	-0.5587	0.67000E+00	1.6170	-0.49597E+00	0.26981E+00
17	0.1575	0.28400E+00	1.0000	-0.28947E+00	0.41335E+00
18	0.	0.	1.0000	-0.16780E+00	0.41335E+00

TABLE II

Meridional Ray Trace from 15 mm Radius at -6.31 Degrees

SURF	C	T	N	Y	UN
0	0.	0.10000E-03	1.0000	0.59005E+00	-0.11000E+00
1	0.1786	0.20000E+00	1.5167	0.58664E+00	-0.10828E+00
2	-0.2969	0.10000E+00	1.0000	0.57359E+00	-0.26044E+00
3	-0.4454	0.50000E-01	1.6475	0.55221E+00	-0.51741E-01
4	-0.1107	0.10000E+00	1.0000	0.54691E+00	-0.12515E+00
5	0.1852	0.20000E+00	1.5167	0.52898E+00	-0.11594E+00
6	-0.2903	0.10000E+00	1.0000	0.51319E+00	-0.25973E+00
7	0.	0.47500E+01	1.5170	0.47644E+00	-0.17011E+00
8	0.	0.95300E+00	1.0000	-0.33954E+00	-0.25973E+00
9	0.3567	0.87000E-01	1.6490	-0.61067E+00	-0.63863E-01
10	0.8732	0.56500E+00	1.5170	-0.62381E+00	-0.13477E+00
11	-0.5858	0.16000E-01	1.0000	-0.65642E+00	0.12190E-01
12	0.2864	0.10900E+00	1.6490	-0.65387E+00	0.51884E-01
13	0.7032	0.61100E+00	1.5170	-0.63760E+00	0.46563E-01
14	-0.4677	0.20000E-01	1.0000	-0.62045E+00	0.23764E+00
15	0.5587	0.57200E+00	1.5170	-0.57070E+00	0.26729E+00
16	-0.5587	0.67000E+00	1.6170	-0.45580E+00	0.23184E+00
17	0.1575	0.28400E+00	1.0000	-0.28222E+00	0.35043E+00
18	0.	0.	1.0000	-0.18670E+00	0.35043E+00

traces show an exit pupil of 9.702 mm and an eye relief of 7.21 mm for the 0.6 zone of the objective lens.

One interesting item is that reversing the eyepiece from its intended design orientation yields a good spacing 0.953 inches (24.2 mm) between the last surface of the Porro Prisms and first surface of the eyepiece. Potential problems, arising from real optical/mechanical tolerances and infinity focusing are thereby alleviated.

3. Ray Traces - Eyepieces Normal Mode

Analysis of the Muffoletto design, with the eyepiece placed in the originally intended orientation, yields the following calculated parameters:

Exit Pupil	= 9.69 mm
Eye Relief	= 24.8 mm
Prism minimum unvignetted aperture	= 33 mm
Unvignetted half-field	= 6.8 degrees

Table III shows the extreme unvignetted ray trace through this system. Table IV shows a -10 degree ray passing nearly through the center of the lens. Unlike the previous design, where no energy 10 degree off-axis passed through the system, all -10 degree off-axis rays from the center to a -15 mm zone is transmitted. Conversely, all +10 degree rays from 0 to +15 will also be transmitted. Whereas the previous design was angularly limited in field extent due to the vignetting of the first element of the eyepiece, this arrangement will be field limited by the physical size of the prisms.

Off-axis transmission in the original design falls to zero at 9.5 degree half angle, while with the eyepiece in the forward orientation, the transmission is approximately 50 percent of full aperture at a 10 degree half angle.

Table IV also shows what the effect of field angle is on eyepiece size. Notice that surface 12, the first surface of the middle doublet of the eyepiece, the -10 ray requires a clear radius of 0.813 inches. Reducing the size of eyepiece elements to reduce overall weight has the effect of reducing the effective aperture at the wide angular field. It should be clear that reducing the diameter of the objective lens does little to reduce the required diameter of the eyepiece elements, since the element clear diameter is primarily determined by the wide field angle requirement.

Placing the eyepiece in the conventional manner reduces the spacing between the last surface of the Porro Prism and the first surface of the eyepiece. Optical and mechanical tolerances in this configuration are therefore more critical.

6

TABLE III

Un-Vignetted Ray Trace for −6.8 Degree Ray at a Radius of .59033 Inches

SURF	C	T	N	Y	UN
0	0.	0.10000E-03	1.0000	0.59005E+00	-0.12000E+00
1	0.1786	0.20000E+00	1.5167	0.58633E+00	-0.11486E+00
2	-0.2969	0.10000E+00	1.0000	0.57246E+00	-0.27080E+00
3	-0.4454	0.50000E-01	1.6475	0.55009E+00	-0.57914E-01
4	-0.1107	0.10000E+00	1.0000	0.54417E+00	-0.13523E+00
5	0.1852	0.20000E+00	1.5167	0.52486E+00	-0.12233E+00
6	-0.2903	0.10000E+00	1.0000	0.50804E+00	-0.26903E+00
7	0.	0.47500E+01	1.5170	0.47008E+00	-0.17612E+00
8	0.	0.29430E+00	1.0000	-0.37525E+00	-0.26903E+00
9	-0.1575	0.67500E+00	1.6170	-0.45195E+00	-0.19306E+00
10	0.5587	0.57900E+00	1.5170	-0.60681E+00	-0.23297E+00
11	-0.5587	0.20000E-01	1.0000	-0.68504E+00	-0.14899E+00
12	0.4677	0.61140E+00	1.5170	-0.72766E+00	0.28003E-01
13	-0.7432	0.11000E+00	1.6490	-0.71959E+00	-0.21284E-01
14	-0.2564	0.16000E-01	1.0000	-0.72446E+00	0.10381E+00
15	0.5858	0.56510E+00	1.5170	-0.69927E+00	0.21430E+00
16	-0.8772	0.87000E-01	1.6490	-0.65376E+00	0.13127E+00
17	-0.3567	0.07000E+00	1.0000	-0.69436E+00	0.36741E+00
18	0.	0.	1.0000	-0.19657E+00	0.36741E+00

TABLE IV

Ray Trace of -10 Degree Ray Near Objective Lens Center

SURF	C	T	N	Y	UN
0	0.	0.10000E-03	1.0000	0.	-0.17434E+00
1	0.1786	0.20000E+00	1.5167	-0.17576E-04	-0.11439E+00
2	-0.2969	0.10000E+00	1.0000	-0.22987E-01	-0.17039E+00
3	-0.4454	0.50000E-01	1.6475	-0.44145E-01	-0.11022E+00
4	-0.1107	0.10000E+00	1.0000	-0.45705E-01	-0.17887E+00
5	0.1852	0.20000E+00	1.5167	-0.63875E-01	-0.11347E+00
6	-0.2943	0.10000E+00	1.0000	-0.86500E-01	-0.15935E+00
7	0.	0.47500E+01	1.5170	-0.10275E+00	-0.10479E+00
8	0.	0.29430E+00	1.0000	-0.64234E+00	-0.15935E+00
9	-0.1575	0.67000E+00	1.6170	-0.64437E+00	-0.13733E+00
10	0.5587	0.57200E+00	1.5170	-0.76523E+00	-0.18147E+00
11	-0.5587	0.20000E-01	1.0000	-0.80361E+00	-0.25706E-01
12	0.4677	0.61100E+00	1.5170	-0.81316E+00	0.12059E+00
13	-0.7032	0.10000E+00	1.6490	-0.78741E+00	0.53997E-01
14	-0.2864	0.16000E-01	1.0000	-0.77335E+00	0.24509E+00
15	0.5353	0.56500E+00	1.5170	-0.70908E+00	0.30794E+00
16	-0.3772	0.57000E-01	1.6490	-0.64123E+00	0.21170E+00
17	-0.3567	0.97800E+00	1.0000	-0.59377E+00	0.53446E+00
18	0.	0.	1.0000	0.22784E-01	0.53446E+00

4. Prisms

Report #1 in Appendix A adequately discusses the various types of erecting prism systems and shows that Porro Prisms are best for the erecting system. A normal version of the Porro Prism erecting system employs two right angle prisms placed at 90 degrees to one another (See Report #1, Appendix A, Figure 13.33). This version of the Porro design leads to a mechanical interference between the eyepiece and the side of one prism with the eyepiece used in the normal configuration. A second version called the Abbe-Porro design is shown in Figure 2. This configuration has identical optical characteristics with those of the normal Porro design but eliminates the mechanical interference problem.

Optical ray traces show that for the very wide field angles, all rays will not be totally internally reflected at the reflecting surfaces of the prism assembly. Each of the four reflecting surfaces are therefore coated with an evaporated layer of aluminum. All surfaces except the entrance and exit aperture were sprayed with black lacquer for stray light reduction and mechanical protection.

After placing the order for the prism, it was discovered that these prisms were no longer available from surplus stock but were now built by the optical section of Jaeger. Since these prism assemblies are cemented, centering alignment cannot be adjusted after assembly. Jaegers had no alignment procedure other than placing the elements on a flat plate while glue dried. Since collimation is critical to binocular systems, alignment of the prism elements prior to cementing to assure no vignetting due to the prism relative position is essential. This alignment was performed in-house using a laser reference beam during the cementing process. This procedure will be described in the section on alignment.

5. Objective Lens

Specifications of the triplet objective radii and spacings were given in Report #2 of Appendix A. The necessary clear radius of each element was determined by the ray trace of 10 degree off-axis rays striking the objectives at a 15 mm radius. Tolerances were specified as $\pm$ 0.005 inches in thickness, $\pm$ 0.003 inches in diameter, 0.25 percent on each radius and optical/mechanical axis to be aligned within 5 min of arc. Each element was coated with ¼ wave of MgF_2 to reduce reflective losses.

An anodized aluminum cell is used to hold the three elements co-axial and at the proper element spacing. The design details as well as the two lens elements spacers are shown in Figure 3. The cell is in turn screwed into the cover of the prism housing.

Abbe's Modification of the Porro Prism System.   This prism system consists of two prisms cemented together. It will invert and revert the image. The system is a direct vision prism but the line of sight will be displaced by the amount d.
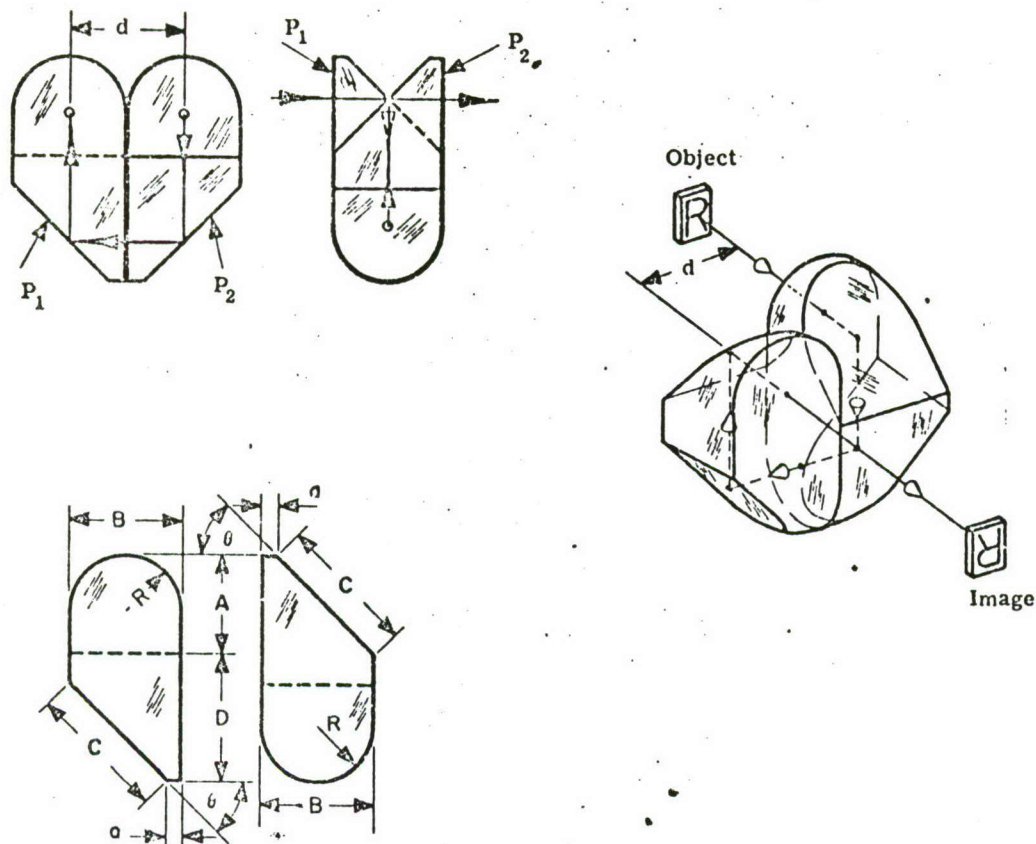
A = 1.00   n = 1.5170 θ = 45° a = 0.10   (chosen arbitrarily)   B = A + a = 1.10
C = 1.4142A = 1.4142   D = A + 2a = 1.20 · R = B/2 = 0.55   d = B = 1.10   t/n = 3.0323
t = 2 (2A + 3a) = 4.60

Figure 2a – Abbe prism system.

Prism #1   Prism #2

Figure 2b – Abbe prism system tunnel diagram.

10
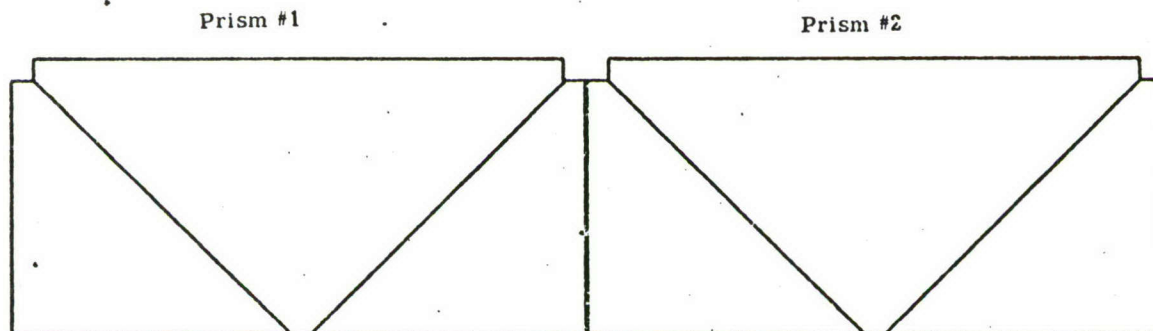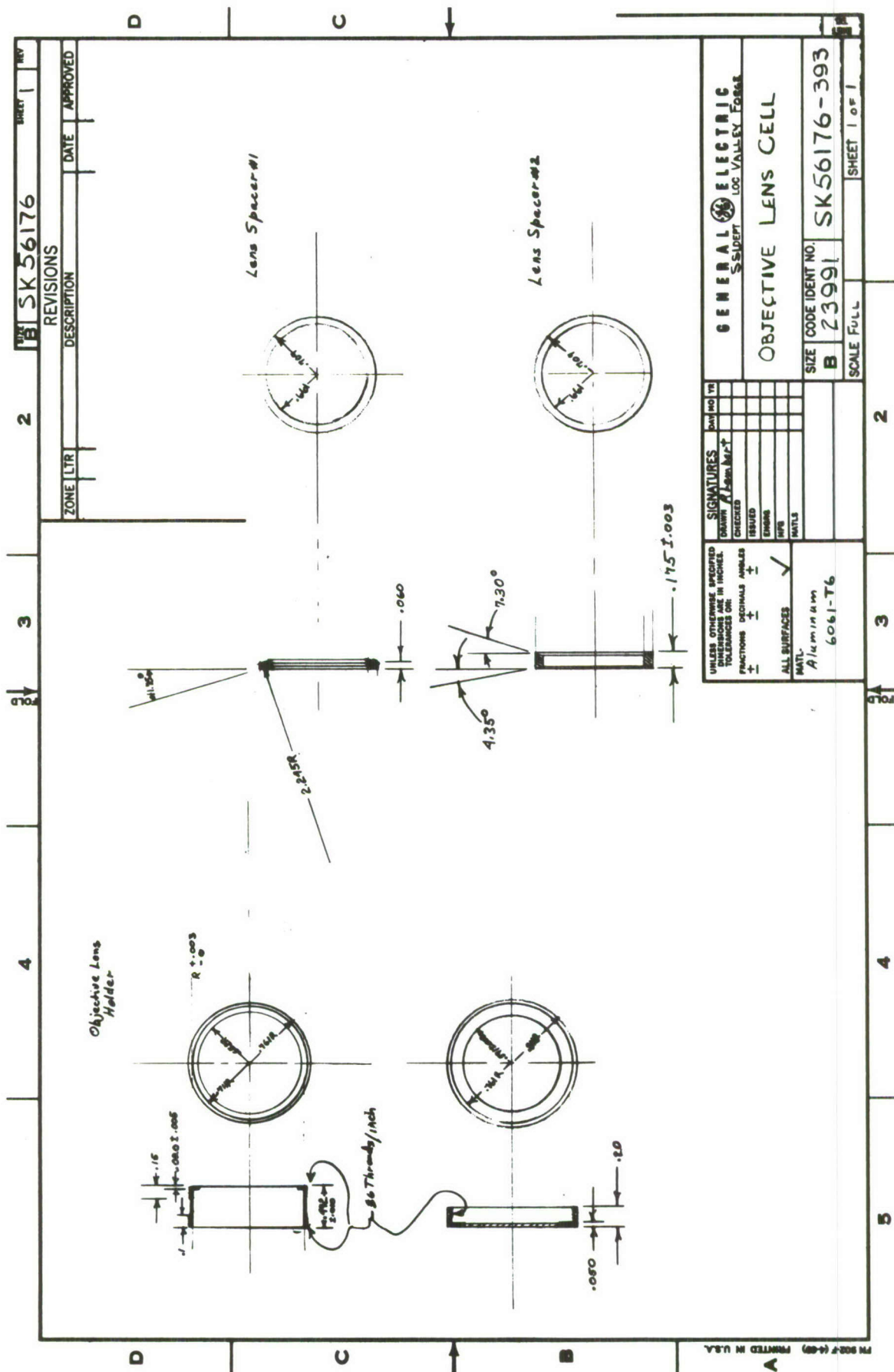
Figure 3 - Lens Cell

6. Prism Housing

Figure 4 shows the details of the support housing for the prism assembly.
There is a right and left hand housing, connected by a hinge. The hinge is
positioned so as to change interpupillary distance of the eyepiece as the
housings are rotated. A maximum spacing of 82 mm and a minimum of 64 mm
is provided limited by the diameter of the eyepiece housings.

The black anodized aluminum housings have two mounting pads machined
into the inner walls and a third machined just above the geometrical center
of the housing. These pads serve as the mounting points for holder of the
prism assembly. The holder or "basket" assembly was fabricated from 0.020
inch stainless steel sheet. Mounting tabs are welded to each "basket" end.
The third tab is part of the bar passing between the two top prisms which
is attached at each end to the "basket." Two set screws in the bar force
the prism assembly solidly into the "basket" locking the assembly in place.
Tubular shims, one on each mounting pad, are cut to length as required to
adjust tilt of the "basket"/prism assembly for final alignment. Figure 5
shows the components of one side of the binocular.

7. Eyepieces

Erfle eyepieces in housing mounts were directly available. Ray tracings
indicated that virtually all the glass was necessary to provide high through-
put at the large off-axis angles. Each eyepiece is individually adjusted for
best focus. A very long eye relief allows the user to wear eyeglasses while
using the binocular; however, eyecups proved to be necessary to maintain the
eye at the exit pupil. Three types of eyecups were provided: flared,
reversed cone and asymmetric. The standard flared cups proved to be un-
comfortable due to little nose room between eyecups. The asymmetric pair
required a special mount which could be easily counterotated with respect
to the eyepieces. The reversed cone pair gave good nose room, but tended
to be somewhat uncomfortable if pushed against the eye socket. Since they
were symmetrical, focusing was very conveniently achieved. The user is
free to choose which set is most comfortable.

To verify the computer ray tracing results, one set of eyepieces was modified
so that they could be used in the original Muffoletto configuration. Knurled
rings or eyecups were not provided for this set.

ALIGNMENT AND TESTING

1. Prism Alignment Cementing

Prism alignment was accomplished using a He-Ne laser beam and two screens
placed perpendicular to one another with each approximately 12 feet from
the alignment fixture. One screen was physically on the ceiling, the other
returned the beam to the laser via a retro-reflecting mirror. A plumb line
from the ceiling was used to position a beam splitter which reflected half
the energy through the base prism to the ceiling target. The base prism was
held in a two-axis mount whose tilt was controlled by micrometer drives.
Tilt adjustment positioned the base prism perpendicular to the laser beam.
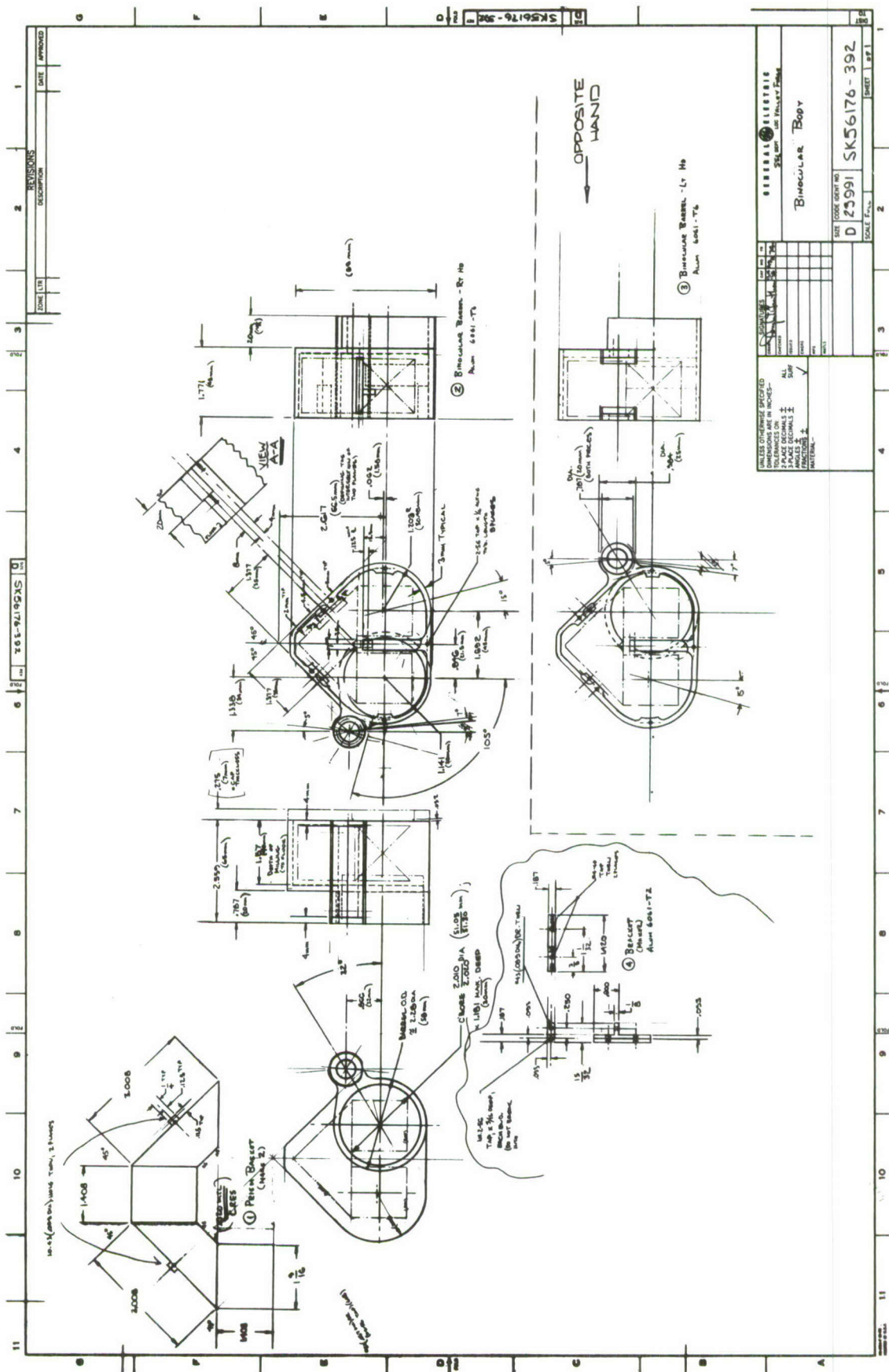The beam splitter was then removed and one prism placed on the base prism.

Figure 4 - Prism Cells

13

Figure 5 - Binocular Components

14

The laser beam image at the ceiling target was positioned by rotation and tilt of the top prism. The prism was cemented in place using UV-71, a UV-setting cement. The second prism was added and the return beam at the laser face was positioned by tilt and rotation of this prism, which in turn was then cemented in place. The return beam was controlled to an angular error of less than 1 milliradian.

2. Collimation

By agreement, collimation specifications Mil-B-8568A (ASG), para, 3,4,5 (b) were applied. The beam from a He-Ne laser was split into two parallel components separately by a convenient interocular space. The direction of the beams were made parallel by retro-reflecting both beams back to the source over a total path length of 400 inches. In this way, the beams were easily co-aligned to within 1 milliradian. The two pencil beams were inserted into the centers of each eyepiece and the reflection from each element's surface co-aligned by translation and rotation of the binocular. The output beams were observed on a reference target approximately 200 inches distant. Reference marks corresponded to the zero positions of the two pencil beams and the centers of the objective lens. The two exit beams were adjusted to fall on the objective center references within 1.12 milliradians convergence, and 2.24 milliradians in divergence in the plane defined by the entrance pencils, and within 1.12 milliradians in the perpendicular direction. The angular specifications translate to linear dimensions of 0.219 inches and 0.438 inches, respectively.

Alignment was an iterative procedure in that the prism was positioned, an objective lens installed and the resulting laser beam position with respect to the reference marks observed. Depending on the direction and amount of misalignment, the appropriate shim length was determined, the monocular disassembled, new shims inserted in the appropriate positions, the system reassembled and another observation of the laser position noted. When alignment is achieved, each of the three retaining screws and all cover screws are cemented with "Lock-Tite" to secure their position in a vibrating environment.

After collimation is achieved, the position and size of the exit pupils were determined by placing the binocular, focusing at infinity, in the output beam of a 12-inch Newtonian collimator. A frosted glass screen was positioned at the best focus by visual observation. The size and diameter of the exit pupils were then measured.

Field of view was measured by observing the source at infinity and rotating the binoculars on an indexing head until the image appears at the edges of the field. A measurement of the respective angular position gives the total angular field. A circular field stop was painted on the exit window of each prism. The diameter of the stop is equal to the width of the prism (32 mm). Without such a stop, the field was square. The corners, at approximately 25 degrees total field angle, were distorted quite badly and therefore not useful. The field stop was incorporated to eliminate this unusual square field.

SUMMARY AND FUTURE WORK

The design of a wide angle, low power binocular system was completed and two units were fabricated. Their characteristics match quite closely the computer predictions. Presently, one unit is undergoing field tests to evaluate the effectiveness of the system when compared to other stabilized and unstabilized reconnaissance optical aids.

High optical efficiency at wide field angles necessitated large optical components in the eyepiece. The present design has high brightness across the entire field of view. Since the eye has a logarithmic power response, it is possible that fairly large vignetting at the field edges may not be objectionable. Smaller elements could reduce the weight of the eyepieces significantly and would thus significantly reduce the overall system weight. The current system weighs too much for operational field usage. Using the present system, the size of the eyepiece components consistent with objectionable vignetting can be empirically determined very readily. The results can be used as inputs for further computer analysis to determine the impact on other optical components within the system.

To further reduce weight, other optical materials such as plastics could be considered. The prisms, since they have no optical power, may be readily changed to low density materials if the optical quality and high transmission can be obtained in large components. Changing the objective lenses or eyepiece components to plastic material would probably require re-design. However, a study should be made to locate good quality, light weight optical materials and a determination made concerning the impact such material would have on the overall design.

APPENDIX

MUFFOLETTO OPTICAL COMPANY, INC.

6100 EVERALL AVENUE

BALTIMORE. MARYLAND 21206

July 16, 1973

R E P O R T # 1

Work Statement #SK-RO-503
Specification #SK-RO-409

Re: P.O. #86HJ-DM-88593-0S,
dated 7/2/73

Investigation of Wide Angle Binocular Prisms:

This report concerns the first preliminary look at the Aberdeen (LWL) 3X binoculars as discussed in the meeting at the Muffoletto Optical Company, Inc. and during discussions between Frank Keisler and our consultant, John Goodell. The principal subject here is the erecting prism type, including arguments for and against various types.

The prism types included are: Porro, Lehman (also called Abbe and Koenig), and Pechan. The main determining factor in prism type in any binocular and especially in the present design is the length to aperture ratio. This determines whether or not the primary image from the objective will fall within or outside the prism.

Design constraints on the present binoculars make this a critical factor. For example, the binoculars are to have at least a twenty degree field of view; the exit pupil must lie 14 millimeters from the eyepiece and have a diameter of 10 millimeters which forces the objective to have a diameter of 30 millimeters. The f/3 system produces (assuming the entrance pupil is coincident with the objective) a 90 millimeter focal length for the objective. Obviously, the optical length of the prism must be less than 90 millimeters.

Consideration of the field of view and aperture indicates approximately a 30 millimeter diameter beam from the objective to the primary focal plane. This means that the prism must have at least a 30 millimeter diameter.

The set of figures indicates various prism types and includes length to aperture ratios. The parameter, t, the tunnel length is the important one to consider. For a Porro pair without truncated edges this ratio is four; for an Abbe the ratio is 5.1962 whether the Abbe is roofed or not; and, for an unroofed Pechan the ratio is 4.6213. Some confusion arises at this juncture concerning a roofed Pechan. Our calculations indicate that a roofed Pechan will have a length to aperture ratio of 6.95.

Obviously, none of these prism types would work if they weren't optically shortened by the refractive index. For an index of 1.5 the Porro shortens to 2.67, the Abbe shortens to 3.4253 and the unroofed Pechan shortens to 3.064.

According to this consideration, the only prisms possible are Porros. There is another possibility however, and that is to use glasses with higher refractive indices. For example Schott Glass SF6 with an index for the D line of 1.805 would reduce the Porro lengths to 2.216, the Abbe lengths to 2.879, and the unroofed Pechan to 2.73. All these lengths are within the f/3 limit.

Note that the Pechan for which the calculations have been made is unroofed. This prism type would only revert (or invert) the image. Reversion and inversion requires either two Pechans in series or a roofed Pechan. Our calculations indicate that a roofed Pechan even with Schott SF6 would have an optical length of 3.850 times its aperture suggesting that a Pechan would not work in an f/3 system or faster system.

John Goodell discussed this with Frank Kaisler and Kaisler suggested a different roof type. Ray tracing found noticeable vignetting with Kaisler's roof. This was pointed out to him.

Frankly, we are a little puzzled here since it has been stated that f/2.5 designs exist with Pechans, contrary to the present findings. It appears that a Pechan would only work if: 1. The system were slower than f/3; 2. The image fell within the prism; 3. Vignetting was allowed.

Allowing the primary to fall within the prism body has the drawback that a field lens would be difficult to insert.

As a result of these calculations, Porro prisms seem to be the best candidate in terms of satisfying the f/3 requirement, the field of view, and the necessary aperture to length ratio. They do not, of course, produce in line images.

We do also have the possibility of using Abbe prisms providing we use glass of high refractive index. This has a possible difficulty that high index glasses almost always have high dispersions. This may or may not rule out prisms with high refractive indices. This will be known only after some preliminary ray tracing. It still must be considered a possibility.
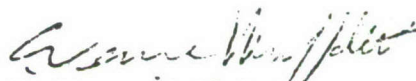
At present we don't see how Pechans can be made to work in f/3 systems without vignetting. So, although they are not completely excluded, they are to be less recommended than the other types.

After a rather extensive search for existing "off the shelf" prisms, we have found a pair of Porro prisms which may work with some modification. No other types (Lehman, Abbe, Koenig, Pechan, etc.) have been found that are adaptable to this system. This, of course, enhances the Porro prism argument even further, at least for use in a preliminary system.

The accompanying figures included descriptions of Porro prisms, Abbe prisms (types A and B), and a Pechan prism. These descriptions come from the Military Standardization Handbook for Optical Design (MIL-HDBK-141.) In addition there are two drawings showing tunnel diagrams for roofed Pechans, including a Descriptive Geometry exercise which indicates vignetting in one type of Pechan roof.

Note from the Military Handbook specification of the Porro that truncating is included in one type of Porro. This is not necessary and increases the optical length, hence is not completely desirable. In the preceeding discussion the shorter, untruncated prism with a length to aperture ratio of four substituted for the truncated version.

MUFFOLETTO OPTICAL COMPANY, INC.

C. Verne Muffoletto
President

13.10.2 Porro Prism System. In 1850 the Italian engineer Porro designed the prism system discussed here. This system consists of two right-angle prisms, usually identical in construction, placed at right angles to each other. It is a direct vision prism system but the axis is displaced by the amount d. This system will invert and revert the image.

Object

Image
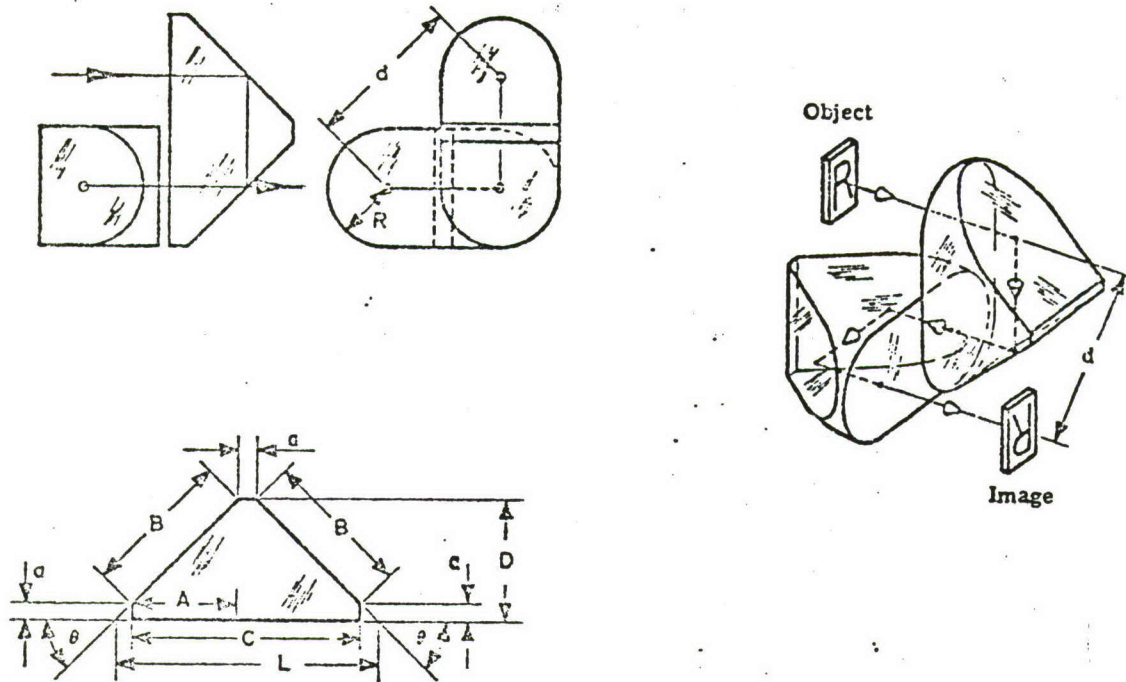
$A = 1.00$ $n = 1.5170$ $\theta = 45°$ (These values are given) $a = 0.10$ (chosen arbitrarily)

$R = A/2 = 0.50$ $B = 1.4142A = 1.4142$ $C = 2A + a = 2.1$ $D = A + a = 1.1$

$L = 2A + 3a = 2.30$ $d = 1.4142 (A + a) = 1.5556$ $t = 2 (2A + 3a) = 4.60$ $t/n = 3.0324$

Figure 13.33-Porro prism system.

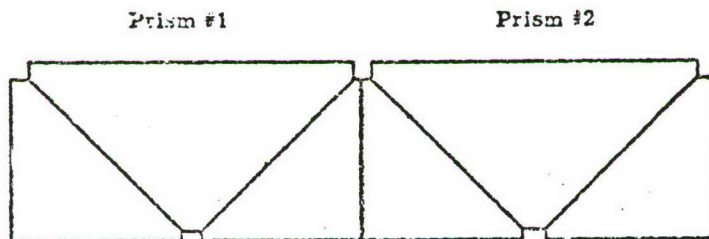Prism #1   Prism #2

Figure 13.34-Porro prism tunnel diagram.

13.10.4 Abbe Prism, Type A.   This prism inverts and reverts the image, but will not deviate the line of sight; hence, it is a "Direct Vision Prism." The prism is made in two pieces which are cemented together.
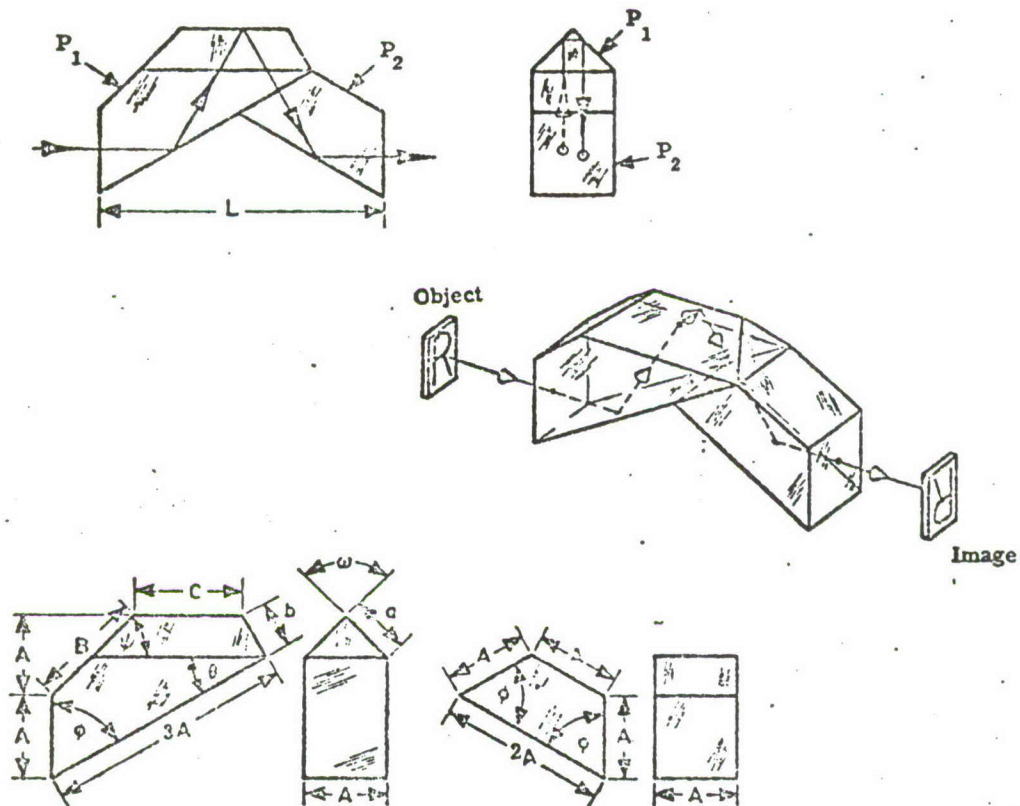
$A = 1.00$ $\theta = 30°$ $\omega = 90°$ $n = 1.5170$ $\varphi = 60°$ $\psi = 45°$ $B = 1.4142A = 1.4142$
$C = 1.3094A = 1.3094$ $a = 0.7071A = 0.7071$ $b = 0.5774A = 0.5774$ $L = 3.4644A = 3.4644$
$t = 5.1962A = 5.1962$ $t/n = 3.4253$

Figure 13.37-Abbe prism, type A.
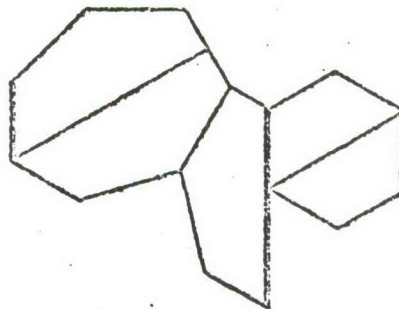
Figure 13.38-Abbe prism, type A, tunnel diagram.

13.10.5 Abbe Prism, Type B. This prism is made of three single units which are cemented together. This prism will invert and revert the image but will not deviate the line of sight. This also is a "Direct Vision Prism."

Prism #2

Prism #1 and 3

Object

Image
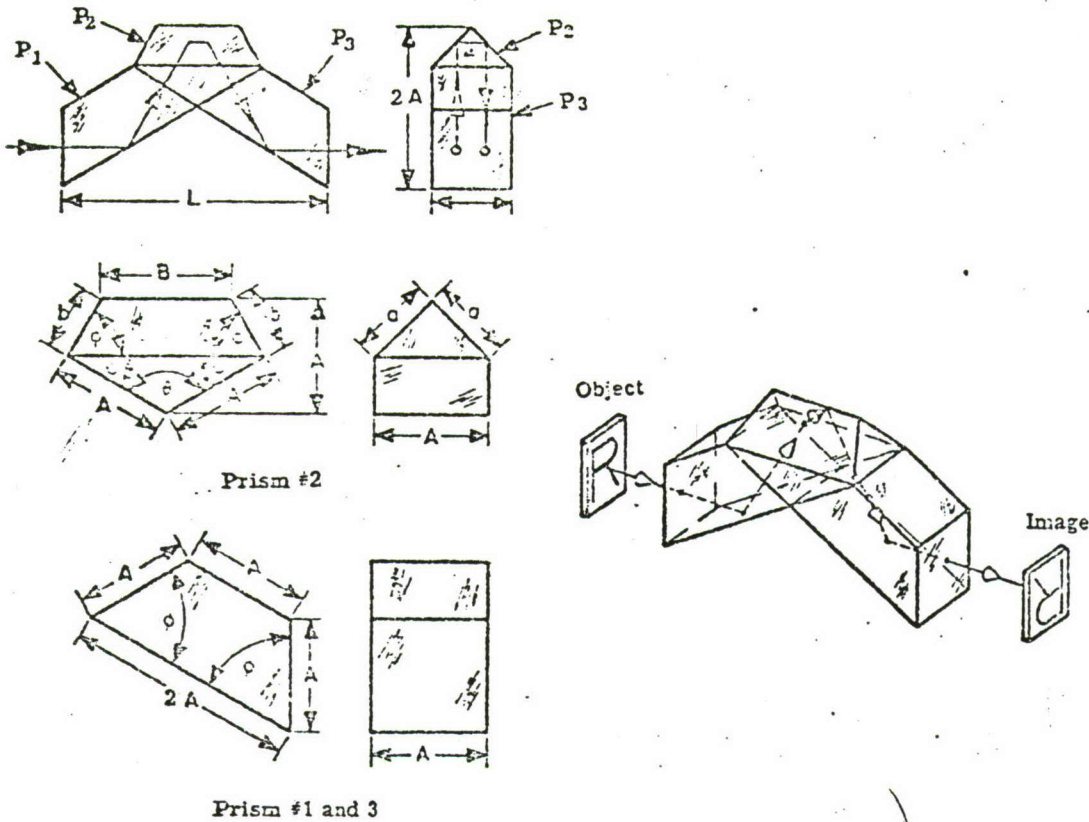
$A = 1.00$ $\theta = 135°$ $\omega = 45°$ $\phi = 60°$ $\psi = 30°$ $n = 1.5170$ $a = 0.7071A = 0.7071$ $t/n = 3.4253$
$b = 0.5773A = 0.5773$ $B = 1.1547A = 1.1547$ $L = 3.4641A = 3.4641$ $t = 5.1962A = 5.1962$

Figure 13.39-Abbe prism, type B.
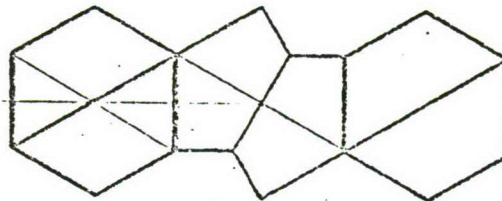
Figure 13.40-Abbe prism, type B, tunnel diagram.

13.10.12 _Pechan Prism._ The prism performs the same duties as the Harting-Dove prism but it has one great advantage over the latter inasmuch as it may be placed in convergent or divergent light. This will permit the reduction in length or height of the instrument. It will invert (as shown) or revert the image, depending on its orientation. It may displace the line of sight if not properly centered but it will not deviate it. The surfaces marked B are silvered and covered with a protective coating. The unsilvered reflecting surfaces of the prism are separated by a distance of about 0.002 inch.

$A = 1.00$ $n = 1.5170$ $\theta = 22° 30'$ $\varphi = 45°$ $\omega = 67° 30'$ $\psi = 112° 30'$ $a = 0.2071A = 0.2071$

$B = 1.0824A = 1.0824$ $C = 1.2071A = 1.2071$ $D = 1.7071A = 1.7071$ $E = 1.8284A = 1.8284$

$t = 4.6213A = 4.6213$ $t/n = 3.0464$
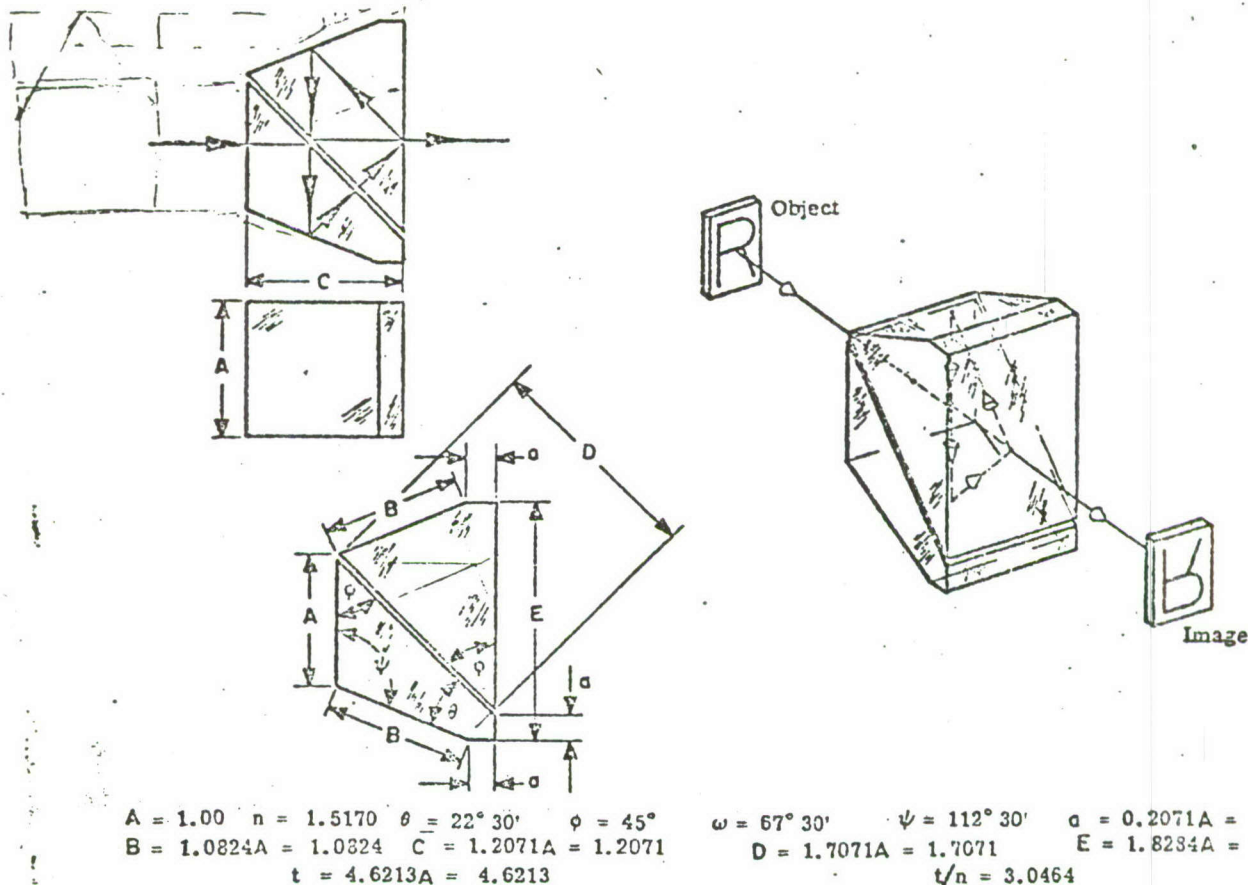
Figure 13.53-Pechan prism.
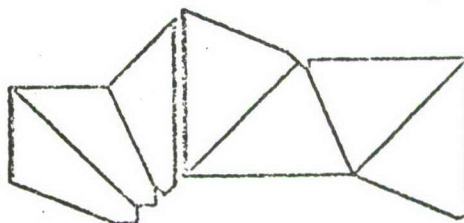
Figure 13.54-Pechan prism tunnel diagram.

$$\frac{\sqrt{2}A}{2}$$

A

A/N
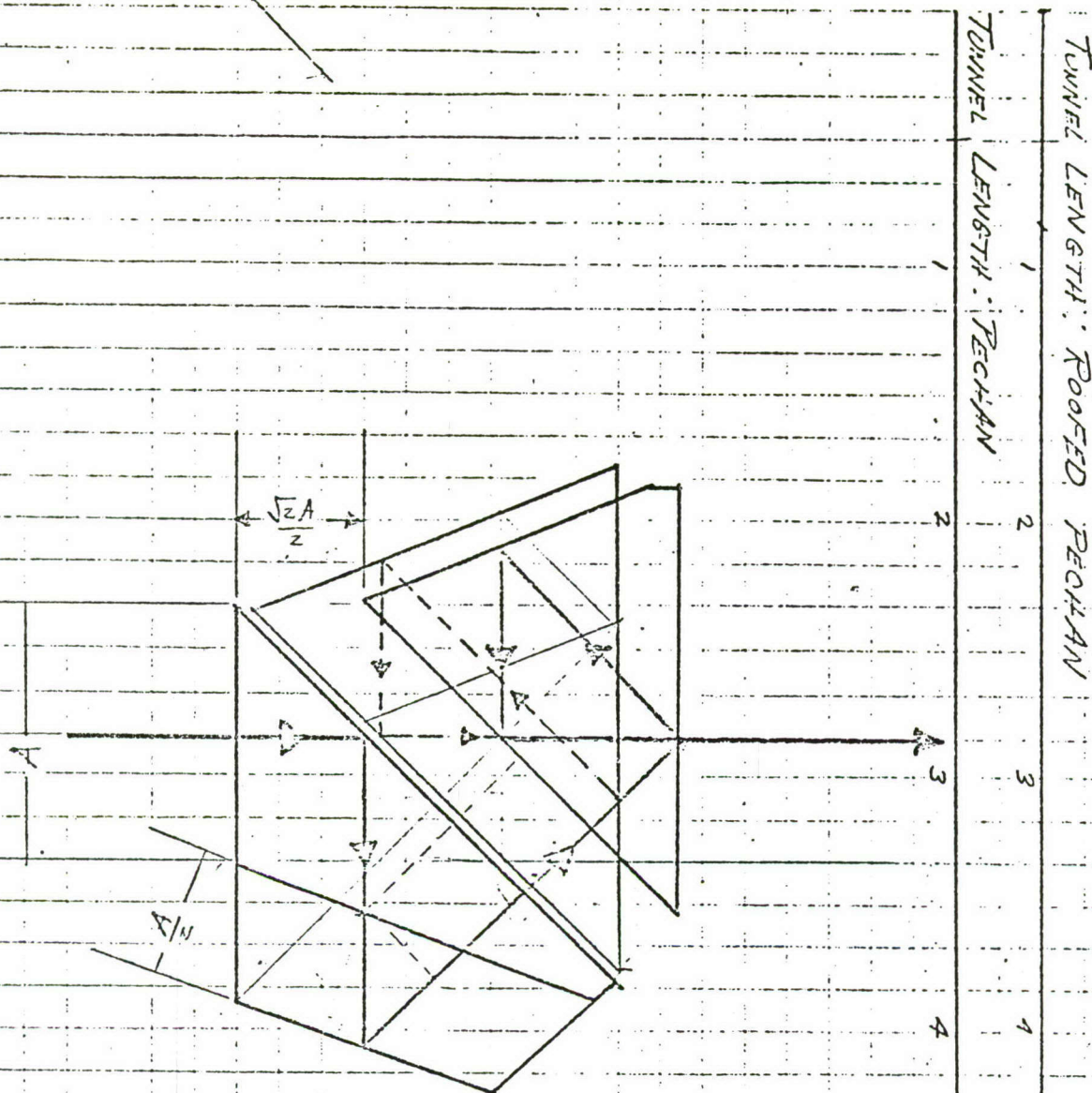
PECHAN WITH A ROOF

$$t \sim 6.95A$$

The smaller prism is the normal prism which is the second of the unroofed Pechan pair. The roof in this case goes across the bottom of the first prism. The shorter vertical line represents the tunnel length, t. The longer vertical line represents the longer tunnel length, corresponding to the roofed Pechan.

The dotted lines indicate the ray path for the larger second prism when it is in contact with the first prism. The solid line through the second prism represents the ray path through the second prism when must be separated from the first prism in order for the optical line of sight to be undeviated.

Descriptive Geometry techniques showing various Pechan faces. The purpose of the view is to show vignetting for the roof type proposed herein. The roof top is at the same height as the top of an unroofed Pechan. The sloping roof sides parallel the 22.5 degree slope of the second prism top. The three rays designated as 1,2, and 3 show that only the ray 1 is not vignetted. The other two rays intersect the second roof plane only <u>after</u> intersecting the prism rear face. Such rays would contribute to the optical image. On the contrary they would appear as scattered light and would reduce contrast.

The rays come from incident rays parallel to the optical axis. Further tracing would show that upper rays are not vignetted in this configuration, but that rays at the bottom of the aperture are cut off. .

Normal view of the plane containing the incident and reflected rays.

Normal view of the roof and edge view of the plane containing the incident and reflected rays

Edge view of the two roof sides.

PECHAN PRISM. Basic view.
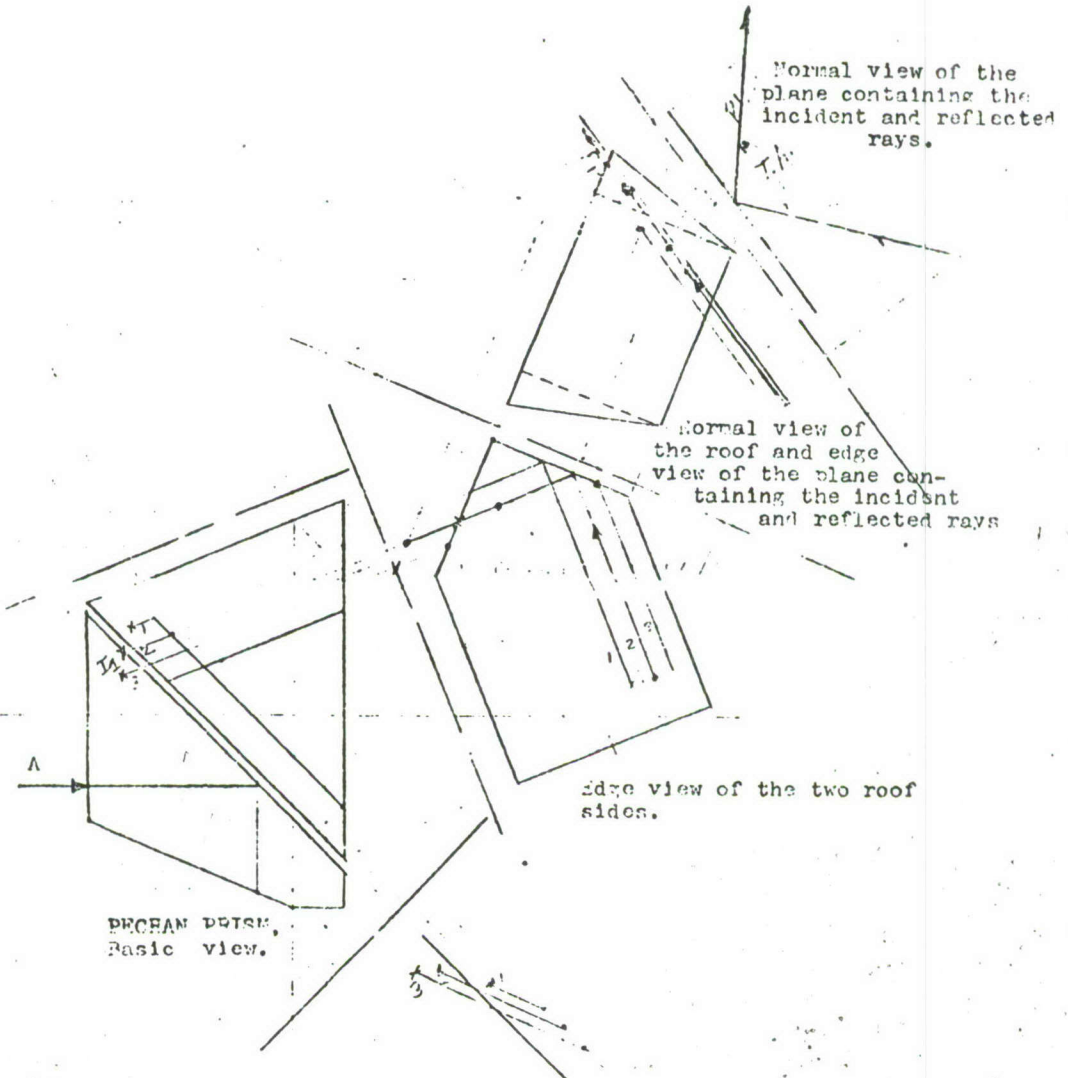
Rays 1,2, and 3 come from incident rays across the prism face at the height shown by the incident ray marked, A

MUFFOLETTO OPTICAL COMPANY, INC.

6100 EVERALL AVENUE

BALTIMORE, MARYLAND 21206

October 9, 1973

R E P O R T # 2

Work Statement #SK-RO-508
Specification #SK-RO-409

Re: P.O. #86HJ-DM-88593-0S,
dated 7/2/73

FINAL DESIGN OF WIDE ANGLE AERIAL RECONNAISSANCE BINOCULARS

DISCUSSION:

This report describes a design for a special binocular type. The design constraints are as follows:

1. Power 3X

2. Field of View .... 20 degrees

3. Exit Pupil Size .... 10 millimeters

4. Eye Relief .... About 10 millimeters

5. Spectral Region .... Total visible

Also, size and weight shall be compatible with hand-held requirements. For economic reasons, the design shall utilize existing components as much as possible.

The accompanying data will show that the design criteria have been met. The power is almost exactly 3X. The eye relief, here determined by the eyepiece, is close to 10 millimeters. The system has been achromatized in the visible spectral region and, over its entire field of view, has a resolution comparing very favorably with that of the human eye (the eye resolves 206 arc seconds.) The device is small and light. The objective and prisms are matched to a Military (probably World War II design) Erfle eyepiece. This reduces cost significantly since it eliminates the need for a new eyepiece design and manufacture, and also makes use of existing prisms. All glasses are common and readily available. All surfaces are spherical or plane.

Report #1, dated 7/2/73, fully investigated erecting prisms and showed why final selection of Porro prisms was made. We have found available Porro

Precision Lenses and Prisms of Glass, Quartz, Fluorite, Silicon, etc.

prisms which can be used by a modification which will reduce the cost to less than one-third the price of new prisms.

After investigating three available Erfle eyepieces, one was selected as clearly the best suited for this application and we were fortunate enough to obtain the design of same (through the efforts of Mr. Frank Kaisler of Westinghouse) from Frankfort Arsenal (see page 4, Lens and Prism Description). This has resulted in cost saving of $1100.00, per page 2 B, 1b cost information of MOC proposal dated 6/21/73. This eyepiece exists completely mounted in a lightweight aluminum focussing mount and may be used "as is." For the sake of greater compactness and some weight reduction, it is possible to de-mount these lenses and reduce their diameters. They can then be re-mounted in a completely new barrel and focussing mount.

Further investigation shows that the center post from existing commercial 10 x 50 binoculars may be utilized to connect both binocular barrels and adjust interpupilary distances. Also, three achromatic doublet lenses were obtained and evaluated for possible use; although the results gave us useful information, we proved that achromatic doublets cannot do this job.

Beyond this, there seems to be no further use of existing parts.

I. THE DESIGN

Table 1.1 lists the vertex locations, radii
and glass types for all binocular elements. Thickness
of each individual element can be derived by subtracting
vertex distances. Thus, the first vertex lies at the coor-
dinate, zero inches, while the second vertex is at the
coordinate .2 inches, indicating a vertex thickness for
the first lens of .2 inches - 0 inches = .2 inches. The
total prism length is 5.5 inches - .75 inches = 4.75 inches.
This includes the total physical ray path through both Porro
prisms.

Note that the Erfle eyepiece has three cemented
doublet combinations. This is indicated by identical
radii and vertex locations.

A triplet comprises the objective primarily
because of the 20 degree field requirement, in order
to avoid sharp curvatures possibly required by off-axis
corrections. The negative element lies between the two
positive elements in order to place the principal plane
near the rear element. This allows the objective focal
plane in these extra wide angle binoculars to fall
beyond the final prism surface.

Figure 1.1 is a full scale drawing of the
telescope with the prism unfolded. The prism length equals
the actual physical length of glass which the light rays
must traverse. The dotted lines in the diagram indi-
cate ray directions in the absence of a prism. The Erfle
eyepiece is shown only in schematic as a block, but to
scale. Note that the telescope will be quite short since

FULL SCALE LAYOUT OF THE 3X BINOCULARS (one side)

ERFLE EYEPIECE
(Block Diagram)

TRIPLET
OBJECTIVE

PRISM(Shown unfolded)

A-A'

B-B'

O'

O

4.75'
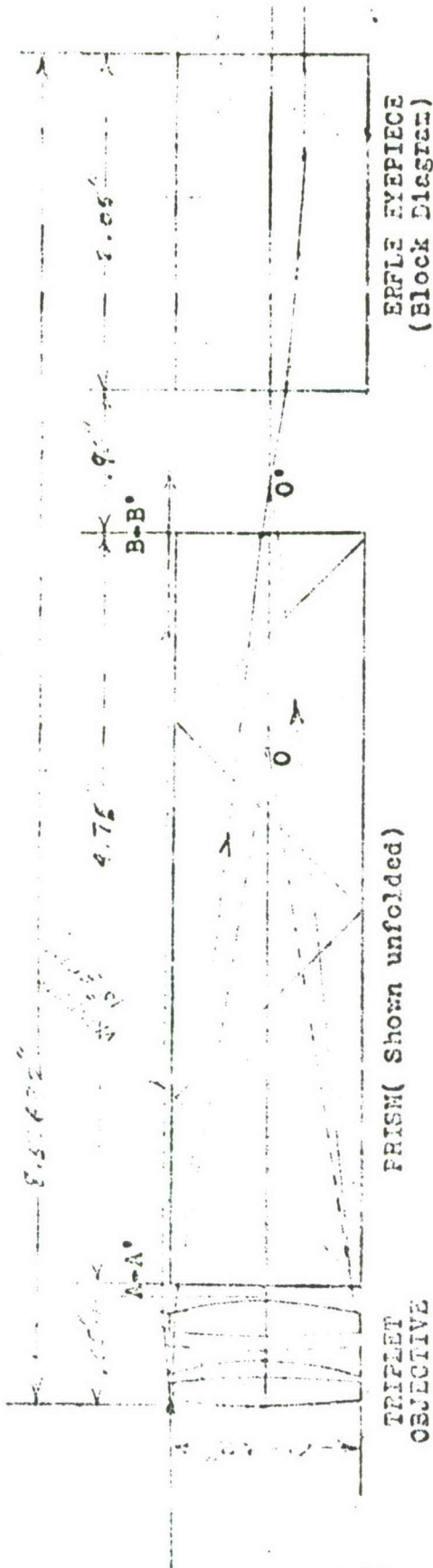
NOTE: In the actual system which uses
two Porro Prisms in the usual
manner the face, B-B' is in the
same plane as the face, A-A'.

In the absence of the prism, the
Triplet focal plane is at the point
O, the intersection of the dotted
rays. The prism extends the focal
plane to the point, O'.
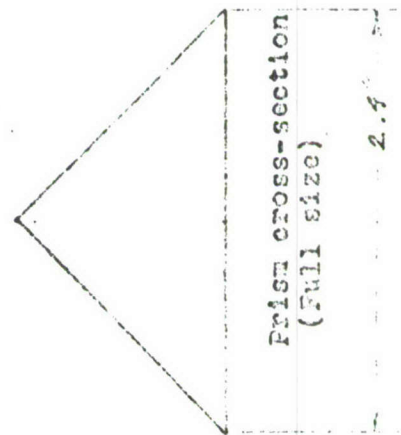
Figure 1.1

BINOCULAR SCHEMATIC

Prism cross-section
(Full size)

2.4'

A-13

LENS AND PRISM DESCRIPTION

	VERTEX LOCATION (in.)	RADIUS (in.)		GLASS
TRIPLET OBJECTIVE	0 .2	5.6 -3.36779	*	BK7 517642
	.3 .35	-2.245 -9.03577	*	SF2 648339
	.45 .65	5.4 -3.44451	*	BK7 517642
PRISM	.75 5.5	inf. inf.	**	BSC2 517645
ERFLE	6.45992 6.54692	2.803 1.14	*	EDF1 649338
	6.54692 7.11192	1.14 -1.707	**	BSC2 517645
EYEPIECE	7.12792 7.23692	3.492 1.422	**	EDF1 649338
	7.23692 7.84792	1.422 -2.138	**	BSC2 517645
	7.86792 8.43992	1.79 -1.79	**	BSC2 517645
	8.43992 8.50692	-1.79 6.347	**	DBC2 617549

* Schott Optical Glass Works, Optical Glasses

** Corning Glass Works, Optical Glasses

Table 1.1

Vertex coordinates, radii, and glass types for all elements of the binoculars.

the prism face, B - B' in the actual device will lie in
the same plane as the face A - A'. A second drawing shows
the prism cross section, assuming a Porro.

A design does not prescribe any specific prism
type. The field of view, however, requires a prism with
a large aperture in order to avoid vignetting at the
field margins. A Porro has the best aperture to length
ratio and therefore appears to be the most suitable prism
for a prototype. It is probably also the least expensive
type.

Table 1.2 is a computer print-out of the ray
coordinates and direction cosines as the input ray, enter-
ing the front surface of the objective at a height of .6
inches (the marginal ray height) traverses each lens
surface and finally leaves the Erfle eyepiece. X is zero
since the ray is meridional. Z is distance along the optic
axis referred to the first lens vertex. Y is the ray
height. L is the direction cosine, here always zero
for the meridional ray. M is the Y direction cosine,
also the sine of the angle the ray makes with the
optical axis. N is the direction cosine along the Z
axis. Positive radii are convex to the incoming ray.
The wavelength is 5893A. The prism can be recognized
easily because the direction cosines entering the prism
are the same as the direction cosines of the ray leaving
the prism. The final output ray height for this mar-
ginal ray is almost exactly 5 millimeters, indicating a

ten millimeter exit pupil.

Table 1.3 resembles Table 1.2 except that the input rays enter the front objective surface at an angle of ten degrees with the optical axis. The Y coordinates in this case indicate the minimum clear aperture required for each element in order to avoid vignetting.

II. PERFORMANCE

1. On Axis.

Figure 2.1 shows four curves corresponding to output ray directions for input rays parallel to the optical axis. The four curves represent output ray directions for the wavelengths 4047A, 4861A, 5893A, and 6563A as indicated. The curves plot output ray direction in milliradians vs. input ray heights up to the .6 inch marginal ray.

In order to generate these particular curves, the best focus was found for the 6563A line. The 4047A rays experience the worst focus, which nevertheless has a spread of the order of the visual angular resolution limit. The output beam divergences for the other rays lie well below the visual angular resolution limit and, in fact, are close to the diffraction limit of the system. Thus the design has been weighted toward the visual spectrum.

2. Five and Ten Degrees Incidence.

Figure 2.2 shows four sets of curves corresponding to output beam directions for input parallel rays making a five degree angle with the optical axis. For clarity each curve has been drawn on a separate graph.

```
X= 0        Y= .6        Z= 3.22356E-2
X= 0        Y= .595796  Z= .14688
X= 0        Y= .584279  Z= .222635
X= 0        Y= .586069  Z= .330973
X= 0        Y= .58383   Z= .431654
X= 0        Y= .578241  Z= .601118
X= 0        Y= .553984  Z= .75
X= 0        Y= 4.76008E-2   Z= 5.5
X= 0        Y=-.109147  Z= 6.46205
X= 0        Y=-.116623  Z= 6.5529
X= 0        Y=-.116623  Z= 6.5529
X= 0        Y=-.170945  Z= 7.10334
X= 0        Y=-.173769  Z= 7.13225
X= 0        Y=-.17832   Z= 7.24815
X= 0        Y=-.17832   Z= 7.24815
X= 0        Y=-.210035  Z= 7.83758
X= 0        Y=-.211349  Z= 7.88044
X= 0        Y=-.200197  Z= 8.42369
X= 0        Y=-.200197  Z= 8.42369
X= 0        Y=-.199212  Z= 8.51005
L= 0        M= 2.04139E-4   N= 1.
```

Table 1.2

Marginal ray height for zero degrees incident ray.

```
YO= .6
X= 0        Y= .605795  Z= 3.28631E-2
X= 0        Y= .6143    Z= .143501
X= 0        Y= .615791  Z= .213895
X= 0        Y= .629916  Z= .326016
X= 0        Y= .655681  Z= .489955
X= 0        Y= .661557  Z= .585873
X= 0        Y= .660272  Z= .75
X= 0        Y= .635752  Z= 5.5
X= 0        Y= .627677  Z= 6.5311
X= 0        Y= .609477  Z= 6.72352
X= 0        Y= .609477  Z= 6.72352
X= 0        Y= .59552   Z= 7.004671
X= 0        Y= .546621  Z= 7.17097
X= 0        Y= .50831   Z= 7.33087
X= 0        Y= .50831   Z= 7.33087
X= 0        Y= .399215  Z= 7.81032
X= 0        Y= .352787  Z= 7.90303
X= 0        Y= .145321  Z= 8.43401
X= 0        Y= .145321  Z= 8.43401
X= 0        Y= .118925  Z= 8.50803
L= 0        M=-.530455  N= .847713
YO
```

Table 1.3

Marginal ray height for ten degrees incident ray.

Figure 2.1

Note: The focus has been adjusted
for best focus at 5563 A.
This has been at the expense
of the 4047 focus.
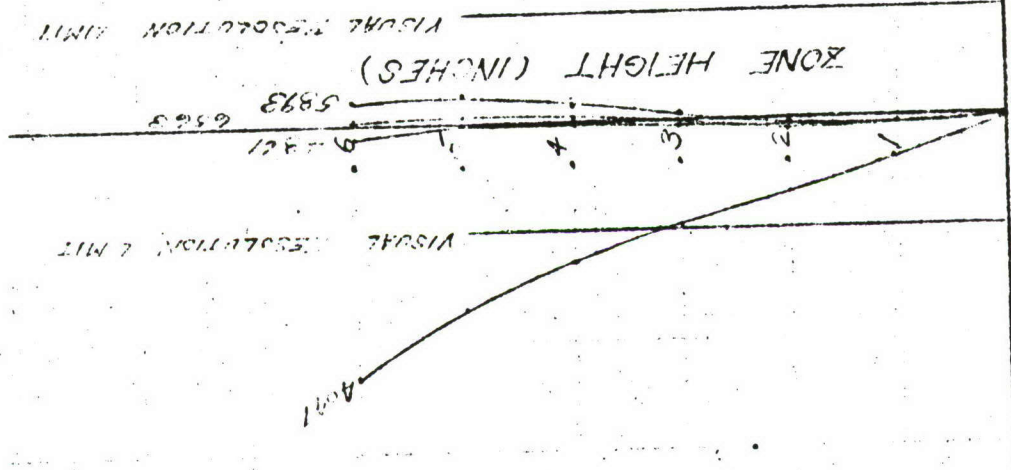
A-18

MERIDIAN RAY HEIGHT (INCHES)

Figure 2.2 EXIT RAY DIRECTIONS AS FUNCTIONS OF RAY HEIGHTS FOR ENTRANCE RAY DIRECTIONS MAKING 5 DEGREES WITH THE OPTICAL AXIS

Note: Both the curves terminate at the
+.2 inch zone due to
vignetting below this zone.

VERTICAL RAY HEIGHT (INCHES)

-6 -5 -4 -3 -2 -1 0 1 2 3 4 5 6

Figure 2.3

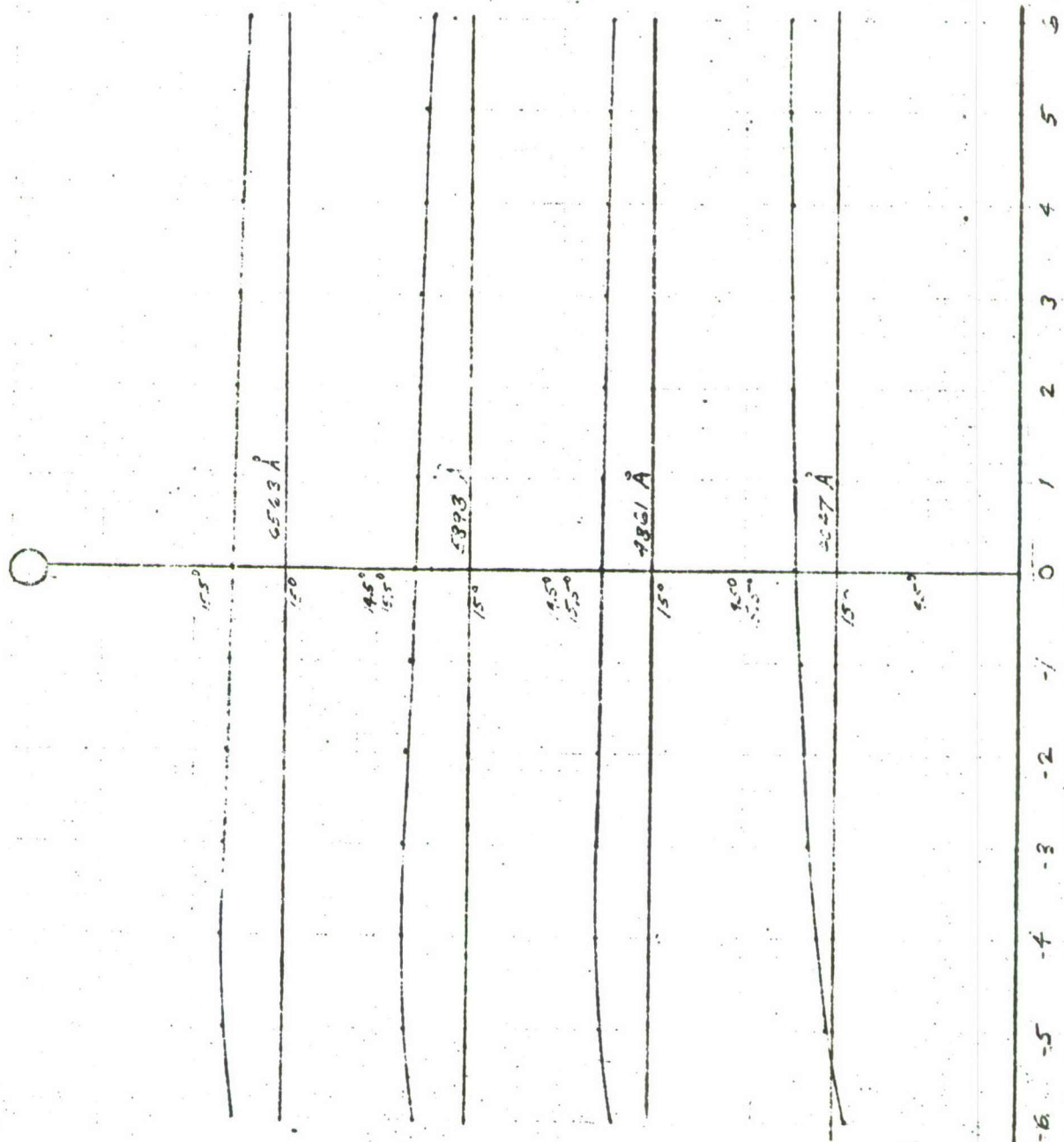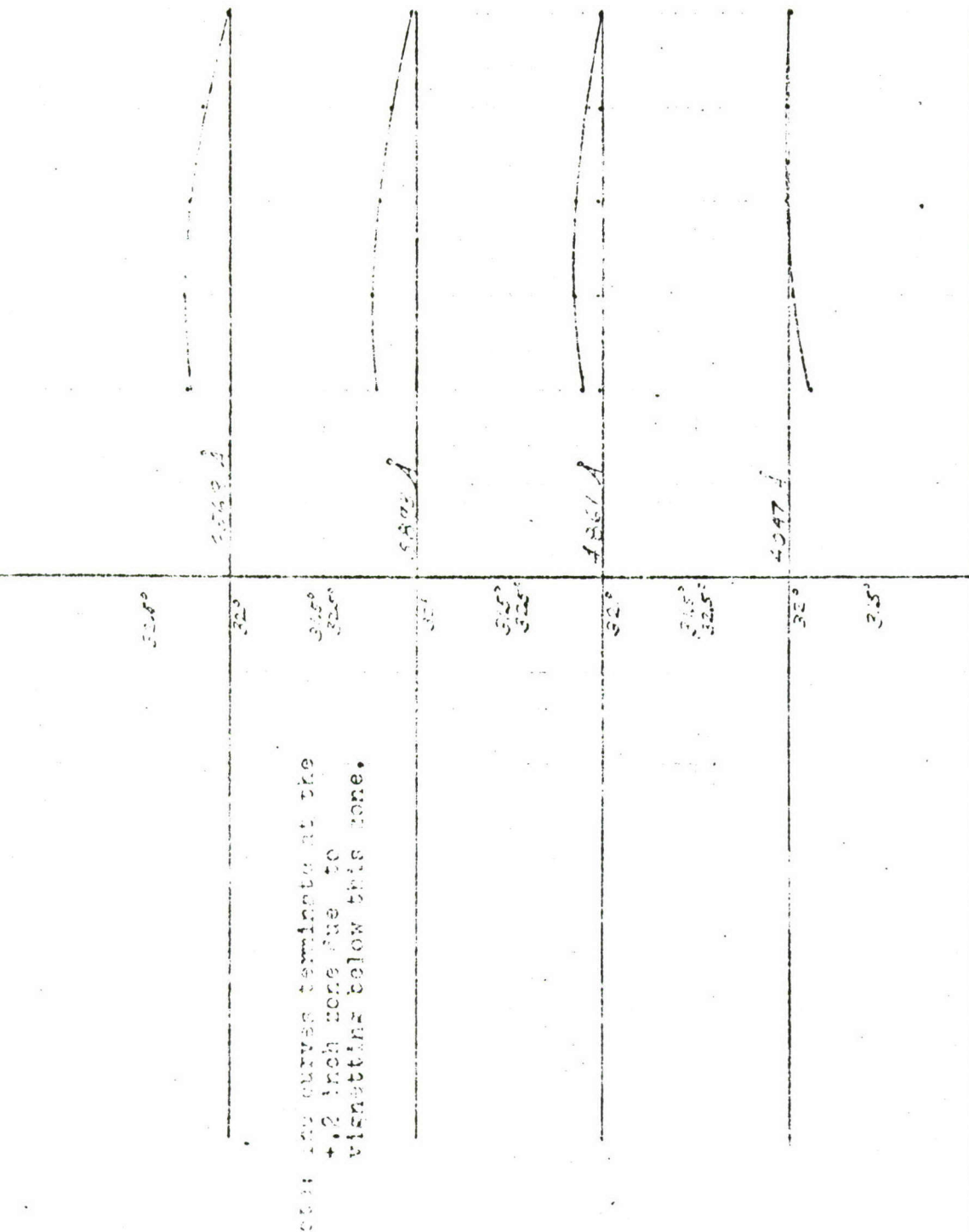OUTGOING RAY DIRECTIONS AS A FUNCTION OF RAY HEIGHT FOR

AN INCOMING PARALLEL RAY BUNDLE AT 10 DEGREES

The coordinates are the heights at which the rays enter the objective lens. The abscissae are the angles which the corresponding output rays make with the optical axis.

Figure 2.3 resembles Figure 2.2 except that the input rays enter the objective at ten degrees with the optical axis. Notice that the curves stop at the .2 inche zone because meridional rays below this height are largely vignetted by total internal reflection at the Erfle internal surfaces.

3. Vignetting.

In the present binoculars, vignetting can result from two causes: physical limitations and total internal reflection when light rays strike internal glass surfaces at angles exceeding critical angles. The effect of the first limitation can be inferred from Tables 1.2 and 1.3 in Section I which show the ray heights of the marginal ray as it intersects each optical surface. An important physical limitation however is the length to aperture ratio of the prism. The prism length is ultimately set by the f number of the system and this in turn sets a limit on the prism aperture.

A more fundamental limitation manifests itself when the field of view becomes large and the eyepiece experiences steep internal incidence angles. For example, a twenty degree incident chief ray becomes a sixty degree emerging ray. Marginal rays experience even steeper slopes. Thus, total internal reflection

occurring when internally incident rays exceed critical angles sets a limitation on field of view which is difficult to circumvent.

Figures 2.4, 2.5, 2.6, 2.7, and 2.8 are computer generated spot diagrams indicating aperture loss arising from total internal reflection. They correspond to 0°, 7°, 9°, 10°, and 12° incident parallel ray bundles. At zero degrees incidence no vignetting from total internal reflection occurs and the corresponding spot diagram is full. At seven degrees, the first loss begins to occur at the bottom and sides of the aperture. Nine degree incident rays show more noticeable loss at the aperture edges and bottom. Ten degree incident rays are quite spotty, indicating that each ray strikes at least one internal surface of the Erfle eyepiece at close to a critical angle. Figure 2.8 depicting aperture loss for 12 degree incident rays shows complete loss of aperture at the bottom edge as well as spotty transmittance throughout the aperture.

III. OPTIMIZATION

The design appears to be close to optimum. Some further design effort, however, has resulted in a slight improvement. This may be academic since the present design seems well within required tolerances; hence further improvement may not even be noticeable. As an example of the degree of improvement, Tables 3.1 and 3.2 compare slightly improved design with the reported

design. The output rays correspond to incoming 5893A rays making an angle of five degrees with the optical axis. Any modifications from the present reported design which result in significant imporvement will be considered in an actual prototype manufacture.

Typical improvements would result in: more tolerance for the lens maker, better resolution (examination of the present design suggests that such modifications would likely produce insignificant improvement to the present design), fewer elements, or smaller and lighter elements.
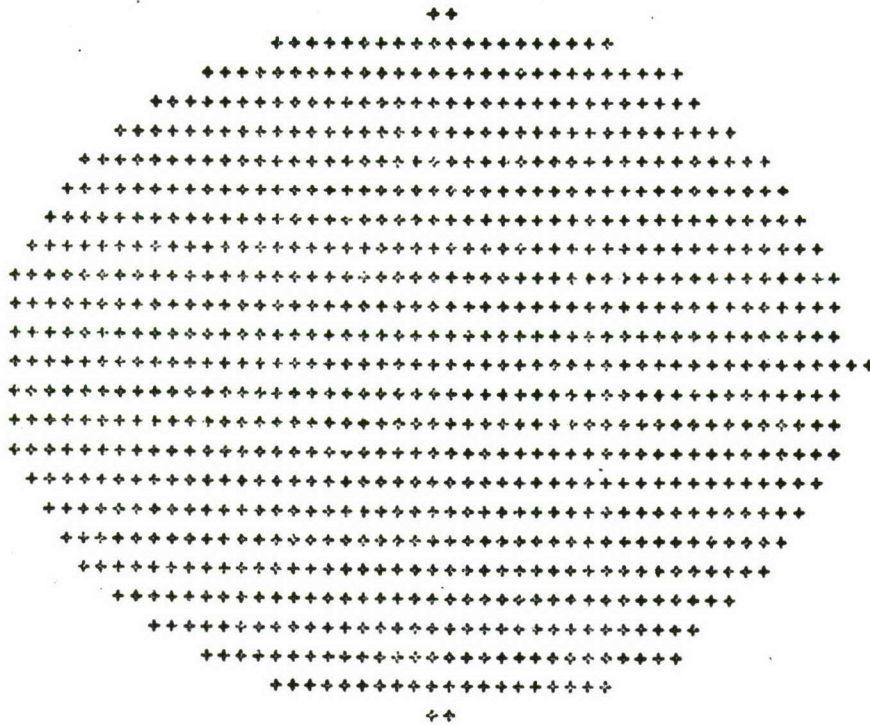
Figure 2.4

Computer generated spot diagram showing aperture for zero degrees
incident rays filling the entrance pupil.
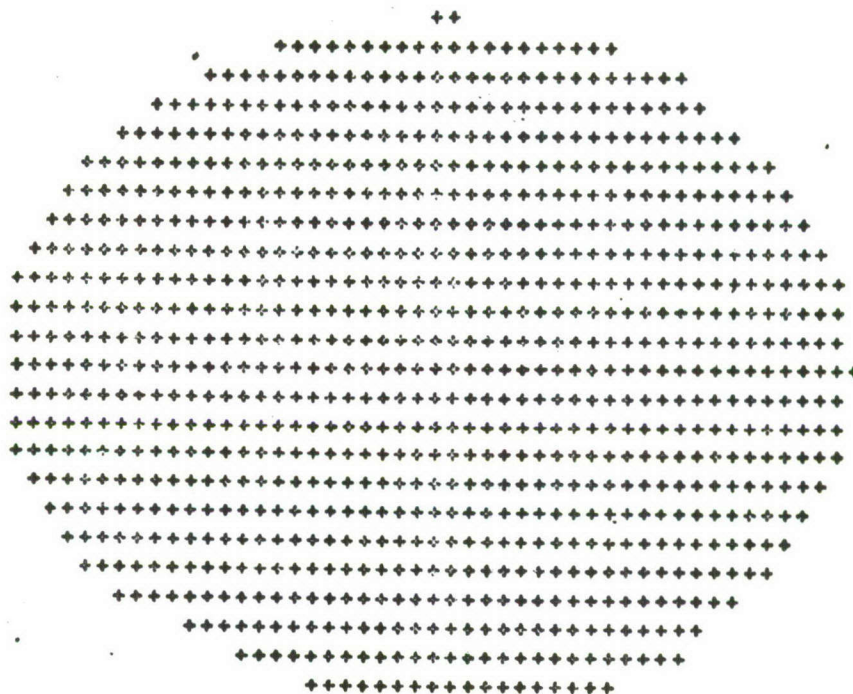
Figure 2.5

Computer generated spot diagram showing aperture for seven degrees
incident rays filling the entrance pupil.
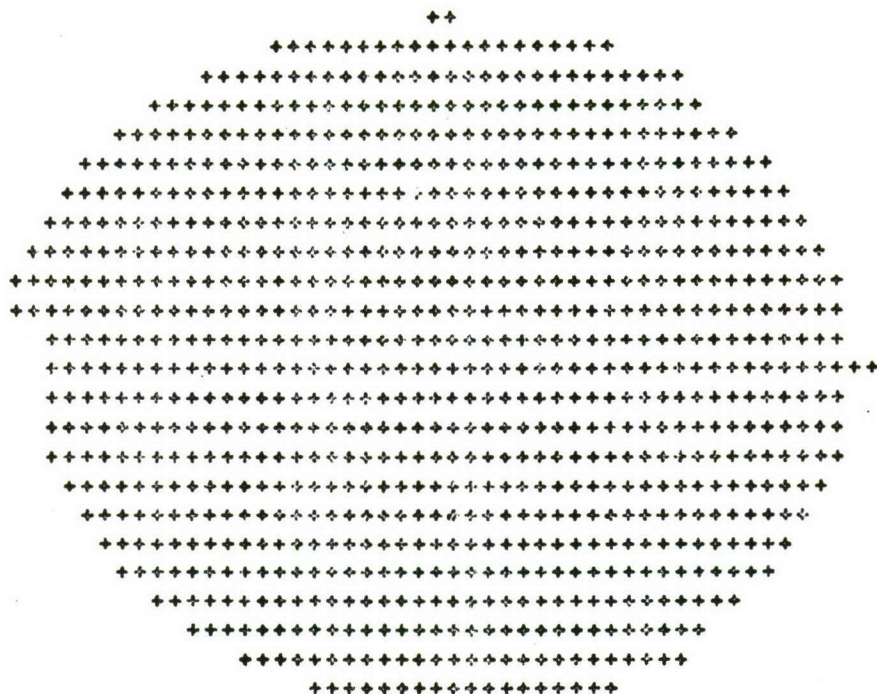
Figure 2.6

Computer generated spot diagram showing aperture for nine degrees
incident rays filling the entrance pupil.
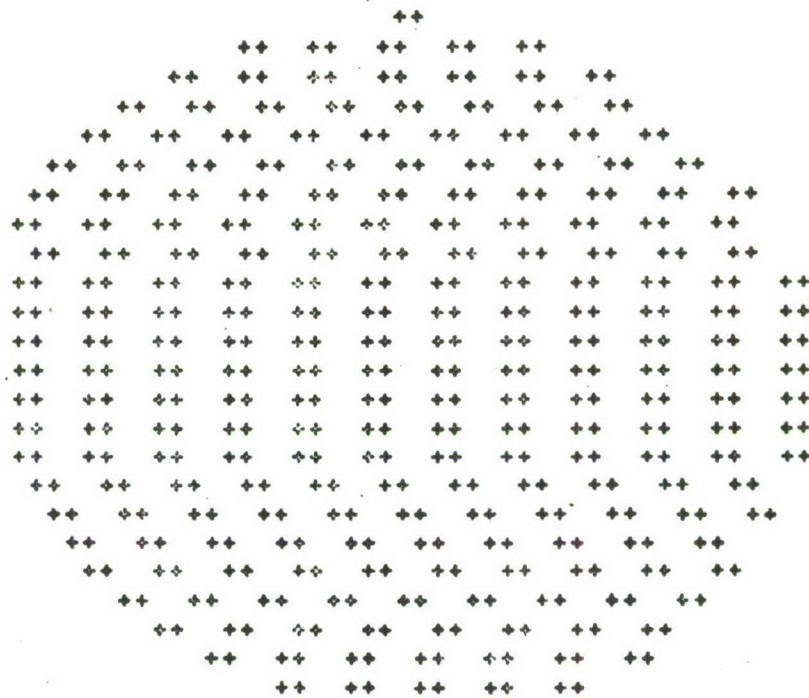
Figure 2.7

Computer generated spot diagram showing aperture for ten degrees incident rays filling the entrance pupil.
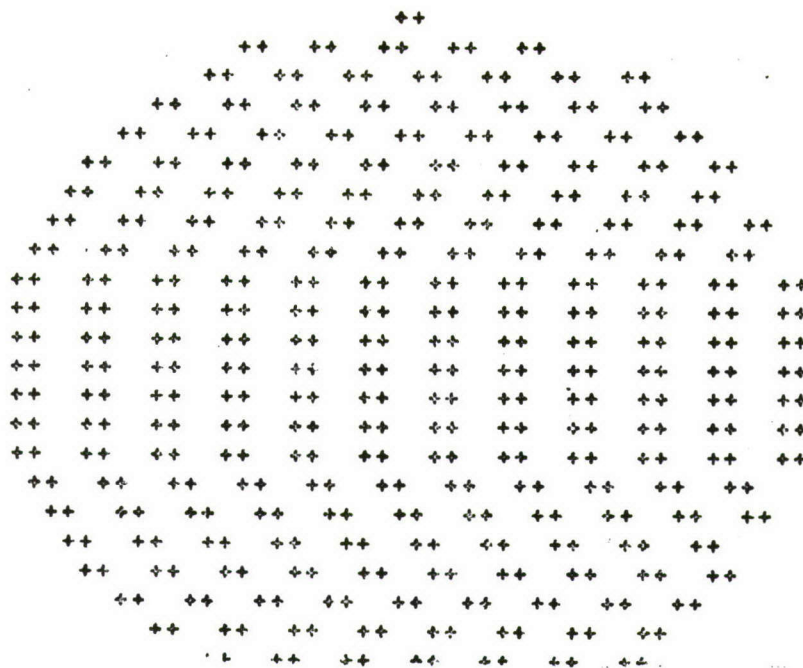
Figure 2.8

Computer generated spot diagram showing aperture for twelve degrees
incident rays filling the entrance pupil.

```
YO= .6
L= 0       M=-.262265 N= .964996
YO= .4
L= 0       M=-.263029 N= .964788
YO= .2
L= 0       M=-.263474 N= .964666
YO= 0
L= 0       M=-.263736 N= .964595
YO=-.2
L= 0       M=-.264012 N= .964519
YO=-.4
L= 0       M=-.264159 N= .964479
YO=-.6
L= 0       M=-.263122 N= .964763
```

```
YO= .6
L= 0       M=-.263909 N= .964548
YO= .5
L= 0       M=-.264052 N= .964509
YO= .4
L= 0       M=-.264144 N= .964483
YO= .3
L= 0       M=-.264162 N= .964478
YO= .2
L= 0       M=-.264115 N= .964491
YO= .1
L= 0       M=-.264029 N= .964515
YO= 0
L= 0       M=-.263931 N= .964541
```

Table 3.1

Output beam angles for correspond-
ing aperture heights. Present design,
radius of fifth triplet surface,
R = 5.4 inches.

Table 3.2

Output beam angles for corres-
ponding aperture heights.
Possibly more optimum design.
Radius of fifth triplet
surface, R = 5.451477124.

DISTRIBUTION LIST

	Copies
Commander US Army Materiel Command ATTN: AMCDL 5001 Eisenhower Avenue Alexandria, VA 22333	1
Commander US Army Materiel Command ATTN: AMCRD 5001 Eisenhower Avenue Alexandria, VA 22333	3
Commander US Army Materiel Command ATTN: AMCRD-P 5001 Eisenhower Avenue Alexandria, VA 22333	1
Director of Defense, Research & Engineering Department of Defense WASH DC 20301	1
Director Defense Advanced Research Projects Agency WASH DC 20301	3
HQDA (ODCSRDA) WASH DC 20310	2
HQDA (DAMO-PLW) WASH DC 20310	1
Commander US Army Training & Doctrine Command ATTN: ATCD Fort Monroe, VA 23651	1

Commander   1
US Army Combined Arms Combat Developments Activity
Fort Leavenworth, KS 66027

Commander   1
US Army Logistics Center
Fort Lee, VA 23801

TRADOC Liaison Office   1
HQS USATECOM
Aberdeen Proving Ground, MD 21005

Commander   1
US Army Test and Evaluation Command
Aberdeen Proving Ground, MD 21005

Commander   1
US Army John F. Kennedy Center for Military Assistance
Fort Bragg, NC 28307

Commander-In-Chief   1
US Army Pacific
ATTN: GPOP-FD
APO San Francisco 96558

Commander   1
Eighth US Army
ATTN: EAGO-P
APO San Francisco 96301

Commander   1
Eighth US Army
ATTN: G-3 O&T Division
APO San Francisco 96301

Commander-In-Chief   4
US Army Europe
ATTN: AEAGC-ND
APO New York 09403

Commander   1
US Army Alaska
ATTN: ARACD
APO Seattle 98749

Commander   1
MASSTER
ATTN: Combat Service Support & Special Programs Directorate
Fort Hood, TX 76544

Commander   2
US MAC-T & JUSMAG-T
ATTN: MACTRD
APO San Francisco 96346

Senior Standardization Representative   1
US Army Standardization Group, Australia
c/o American Embassy
APO San Francisco 96404

Senior Standardization Representative   1
US Army Standardization Group, UK
Box 65
FPO New York 09510

Senior Standardization Representative   1
US Army Standardization Group, Canada
Canadian Forces Headquarters
Ottawa, Canada K1A0K2

Director   1
Air University Library
ATTN: AUL3T-64-572
Maxwell Air Force Base, AL 36112

Battelle Memorial Institute   1
Tactical Technical Center
Columbus Laboratories
505 King Avenue
Columbus, OH 43201

Defense Documentation Center (ASTIA)   12
Cameron Station
Alexandria, VA 22314

Commander   2
Aberdeen Proving Ground
ATTN: STEAP-TL
Aberdeen Proving Ground, MD 21005

Commander   1
US Army Edgewood Arsenal
ATTN: SMUEA-TS-L
Aberdeen Proving Ground, MD 21010

US Marine Corps Liaison Officer   1
Aberdeen Proving Ground, MD   21005

Director   1
Night Vision Laboratory
US Army Electronics Command
ATTN: AMSEL-NV-D (Mr. Goldberg)
Fort Belvoir, VA   22060

Commander   1
US Air Force Special Communications Center (USAFSS)
ATTN: SUR
San Antonio, TX   78243

Commander   1
US Army Armament Command
ATTN: AMSAR-ASF
Rock Island, IL   61201

Mr. Verne Muffoletto   2
Muffoletto Optical Co.
6100 Everall Ave
Baltimore, MD   21206

Commander   4
Frankford Arsenal
ATTN: FCD-O (Mr. Wright Scidmore)
Philadelphia, PA   19137

General Electric   4
Valley Force Space Center
Space Sciences Laboratory (Ray Lambert)
PO BOX 8555
Valley Forge, PA   19101

Westinghouse Electric Corporation   2
Defense & Space Center
Surface Division
Baltimore/Washington Intl Airport
Box 1897
(Mr. Frank Kaisler)
Baltimore, MD   21203